PEOPLE'S DEMOCRATIC REPUBLIC OF ALGERIA

ECHAHID CHEIKH LARBI TEBESSI UNIVERSITY

FACULTY OF SCIENCES AND TECHNOLOGY

FIELD OF STUDY: SCIENCES AND TECHNOLOGY (ST)

Course Handout

Course Title : Applied Geophysics

Specialization: Geotechnics

Level : Master (S1)

Prepared by: Dr. ABDI Abdelmadjid

Academic Year: 2025/2026

Preface

In modern civil engineering, understanding subsurface conditions is essential for the safe and efficient design of foundations, earth structures, and infrastructure. Applied geophysics provides engineers with non-destructive methods to explore, analyze, and characterize the ground before and during construction activities.

This course, part of the Master in Civil Engineering – Specialization: Geotechnics, is designed to introduce students to the principles, techniques, and applications of applied geophysics. It covers gravimetric, electrical, seismic, and electromagnetic methods commonly used in geotechnical investigations, with a focus on their advantages, limitations, and interpretation.

Through a combination of theoretical foundations and practical approaches, students will develop the ability to select appropriate methods, analyze geophysical data, and integrate findings with geotechnical studies to support informed engineering decisions.

This course handout has been prepared in accordance with the recommendations for the harmonization of the Civil Engineering Master's program, Specialization: Geotechnics (2022–2023). It is structured into five (5) chapters, each focusing on a fundamental aspect of applied geophysics:

1. **General Overview of Geophysics and Its Applications**
   This chapter introduces the basic principles of applied geophysics, its role in civil engineering, the physical parameters measured, main prospecting methods, and their advantages and limitations.
2. **Gravimetric and Micro-Gravimetric Methods**
   Covers the principles of gravity-based surveys, measurement techniques, data interpretation, and their applications in subsurface investigation.
3. **Electrical Methods**

Focuses on electrical resistivity and conductivity techniques used to map subsurface properties, including data acquisition, processing, and interpretation.

4. **Seismic Methods**

   Explores seismic wave propagation, refraction, and reflection techniques used to evaluate soil and rock properties for geotechnical and structural projects.

5. **Electromagnetic Methods**

   Presents electromagnetic techniques for subsurface characterization, including ground-penetrating radar (GPR) and related applications in geotechnical site assessments.

Contents

Chapter.1 Fundamentals of Geophysics and Its Applications

I.1 Definition of Geophysics

Geophysics is a branch of Earth sciences that investigates the subsurface by measuring and interpreting its physical properties. It aims to understand the structure, composition, and dynamic behavior of the Earth through parameters such as density, elasticity, resistivity, magnetic susceptibility, and thermal conductivity (Sheriff, 2002, Lowrie & Fichtner, 2020).

I.2 Internal Geophysics

Internal geophysics is concerned with the study of the Earth's deep structure and dynamics. It primarily focuses on:

- The gravitational field
- The magnetic field
- Heat flow and the geothermal gradient
- Seismic wave propagation and the layering of the Earth's interior

I.3 External Geophysics

External geophysics deals with the study of the Earth's outer layers and non-mineral planetary components. Its applications extend to:

- Meteorology and climate analysis
- Oceanography
- Glaciology
- Hydrology and hydrogeology
- Planetology

I.4 Geophysical Techniques and Major Methods

The principal geophysical methods employed for subsurface investigations include:

- Gravimetric methods – measure variations in density and mass distribution.
- Magnetic methods – detect anomalies in the Earth's magnetic field.
- Electrical resistivity methods – evaluate the resistivity and chargeability of subsurface layers.

- Electromagnetic methods – measure the response of the ground to combined magnetic and electric fields.
- Seismic methods (reflection and refraction) – analyze seismic wave travel times, amplitudes, and subsurface layering.
- Well logging techniques – record in-situ physical properties such as resistivity, spontaneous potential, and sonic velocity within boreholes.
- Thermometry (geothermal measurements) – assess heat flow and temperature gradients.

I.5 Physical Properties of Rocks

a) Elastic properties:

The elastic properties of rocks determine how they deform under stress and recover when the load is removed. They are expressed by parameters such as Young's modulus (E), shear modulus (G), and Poisson's ratio (ν). These directly control the propagation of seismic waves. The velocity of **compressional waves (Vp)** and **shear waves (Vs)** is given by:

- P-wave velocity:

$$V_p = \sqrt{\frac{\lambda+2\mu}{\rho}} \tag{1.1}$$

- S-wave velocity:

$$V_s = \sqrt{\frac{\mu}{\rho}} \tag{1.2}$$

where λ and μ are Lamé constants, and ρ is density.

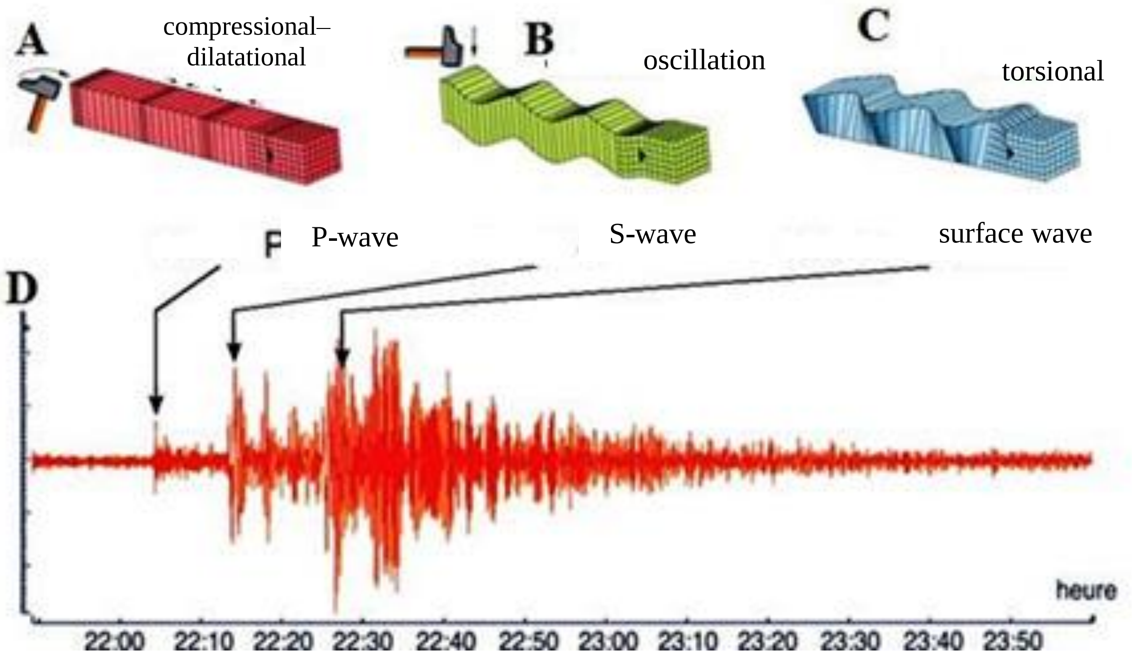

Figure 1. 1 Displacement of particles in a medium through which body waves propagate (A) compression waves, (B) shear and surface waves ,(C) torsional waves and (D) seismic wave arrival times) (Bolt, 1976).

b) Electrical properties:

The response to a current injection depends on the resistivity (ρ), conductivity (σ), and chargeability (M) of the subsurface materials. When an electric current is injected into the ground, the behavior of the system follows Ohm's law, expressed as $U = R\ I$, where R is the resistance. Resistance is defined as $R = \rho\ L/A$, where L is the length and A is the cross-sectional area of the conductor. Substituting this into Ohm's law gives $U = \rho\ I\ L/A$.

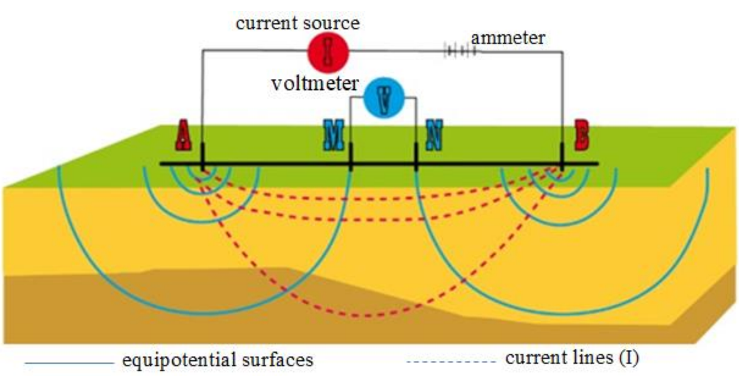

Figure 1. 2 Principle of the geo-electrical method (Chouteau & Giroux, 2006).

c) **Magnetic properties:** Magnetic properties describe how rocks and minerals respond to the Earth's magnetic field. They are mainly governed by the presence and concentration of ferromagnetic minerals such as magnetite, hematite, and pyrrhotite. Variations in magnetic susceptibility and remanent magnetization help identify geological structures, locate ore deposits, and map subsurface features. Magnetic surveys are widely used in geophysics for mineral exploration, structural mapping, and archaeological investigations (Telford *et al.*, 1990, Sharma, 1997).

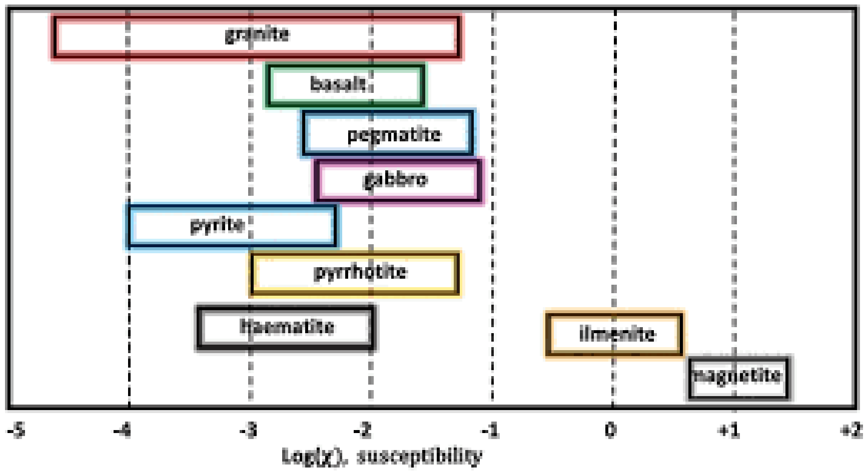

Figure 1. 3 Magnetic susceptibility ranges (Log(χ)) of common rocks and minerals, showing variations from highly susceptibile materials (e.g., granite) to low susceptible minerals (e.g., magnetite).

d) **Gravimetric properties:**

Gravimetric properties refer to the variations in the Earth's gravitational field caused by differences in the density of subsurface materials. These variations, measured in terms of gravitational acceleration (g), provide valuable information about the distribution of rocks, voids, and ore bodies. Gravimetric methods are widely used in geophysics to detect density anomalies, map geological structures, and support mineral and hydrocarbon exploration (Dobrin & Savit, 1960).

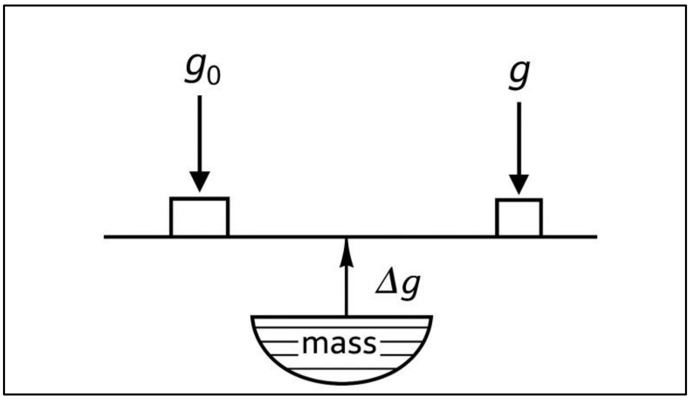

Figure 1. 4 Principle of the gravimetric method, showing the variation in gravitational acceleration (Δg) caused by a subsurface mass (Chouteau & Giroux, 2006).

e) Electromagnetic properties:

The electromagnetic properties of rocks describe how they interact with electromagnetic fields. These include electrical resistivity (ρ), electrical conductivity (σ), dielectric permittivity (ε), and magnetic permeability (μ). These properties control the flow of electric current and the propagation of electromagnetic waves in the subsurface. Their values depend on factors such as mineral composition, porosity, fluid content, and temperature, and they are essential in geophysical methods like resistivity surveys, induced polarization, electromagnetic sounding, and ground-penetrating radar (GPR) (Ward, 1990, Sharma, 1997).

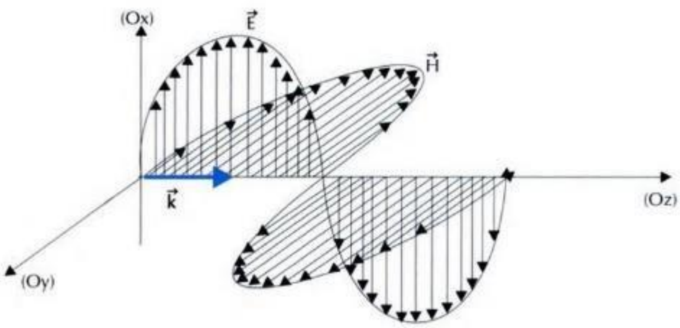

Figure 1. 5 Electromagnetic waves (Chouteau, M. and Giroux, B., 2006).

I.6 Applied Geophysics

Applied geophysics is oriented towards practical and often economically driven goals, such as:

- Mineral and petroleum exploration

- Groundwater detection and aquifer characterization
- Civil and geotechnical engineering (e.g., tunnels, cavities, landslides)
- Environmental investigations (e.g., landfill mapping, contamination assessment)
- Archaeological prospection
- Planetary exploration

I.7 Selection of Geophysical Methods

The choice of a suitable geophysical method depends on:

- The physical contrast between the target and surrounding materials
- Depth, size, and geometry of the anomaly (e.g., cavities, faults, mineralized zones)
- Resolution requirements and investigation depth
- Financial and time constraints
- Sensitivity to environmental and geophysical noise

I.8 Commonly Measured Parameters

- Electrical resistivity (natural and induced)
- Magnetic field intensity
- Gravitational acceleration
- Seismic wave travel time and amplitude
- Electromagnetic field response

Geophysical methods are classified according to the nature of the energy source used and the type of physical property measured. Natural methods rely on existing fields such as gravity, magnetism, or natural electric and telluric currents, while induced methods involve the artificial generation of signals, such as electrical currents, electromagnetic waves, or seismic sources. Each method measures a specific physical quantity—such as gravity acceleration, magnetic field intensity, electrical resistivity, or seismic wave travel time—which is then interpreted to estimate subsurface parameters like density, susceptibility, resistivity, velocity, or impedance. Table I.1 summarizes the main geophysical methods, their measured quantities, and the corresponding parameters of interest.

Table 1 Main Geophysical Methods, Measured Quantities, and Parameters

Type	Method	Measured Quantity	Parameter
Natural	Gravimetry	Gravity acceleration	Density
Natural	Magnetometry	Magnetic field	Susceptibility
Natural	Telluric	Telluric field	Resistivity
Natural	Magnetotelluric	Magnetic field + Telluric field	Resistivity
Induced	Electrical and Electromagnetic	Electrical voltage, EM field	Resistivity
Induced	Seismic Refraction	Travel time	Velocity, Impedance
Induced	Seismic Reflection	Travel time + Wave amplitude	—

Chapter.2 Gravimetric and Micro-Gravimetric Methods

II.1. Introduction

Gravimetry is the science concerned with measuring, analyzing, and interpreting variations in the Earth's gravitational field, as well as that of other bodies in the solar system. It is closely linked to geodesy, which studies the Earth's shape and dimensions. The primary goal of gravimetry is to examine variations in gravity to infer the distribution of mass within the Earth, thereby providing insights into its internal structure and identifying locations of density contrasts in the subsurface.

II.2. The Density of Rocks

A key parameter in gravimetric studies is the volumetric mass, commonly referred to as the density of rocks. Density is defined as the ratio of mass to volume:

$$\rho = \frac{m}{V}$$

where ρ is the density, m is the mass, and V is the volume. Its SI unit is kilograms per cubic meter (kg/m^3), with 1 g/cm^3 equivalent to 1000 kg/m^3. For reference, the density of water at 25°C is 1000 kg/m^3.

Note: In English, “volumetric mass” is called **density**, while what is often termed “density” in other contexts is referred to as **relative density** (Clark, 1966, Carmichael, 2017).

Gravimetry is a fundamental discipline within geophysics, with a wide range of applications. Analysis of gravity variations can help address structural and geodynamic questions, and it is also employed in hydrogeology, volcanology, civil engineering, archaeology, and environmental geology.

Table 2 Density Values of Common Geological Materials

Designation	Density
Pure water	1
"Dry" sand	1.4 to 1.65
"Wet" sand	1.9 to 2.05
Salt	2.1 to 2.4
Marnes	2.1 to 2.6
Limestones	2.4 to 2.8
Granites	2.5 to 2.7
Basalts	2.7 to 3.1
Iron	7.3 to 11.1
Gold	15.6 to 19.4
Oil	0.6 to 0.9

Gravimetry is thus a cornerstone of geophysical investigation, enabling the study of structural, geodynamic, and environmental phenomena by linking measured gravity variations to the distribution of masses beneath the Earth's surface.

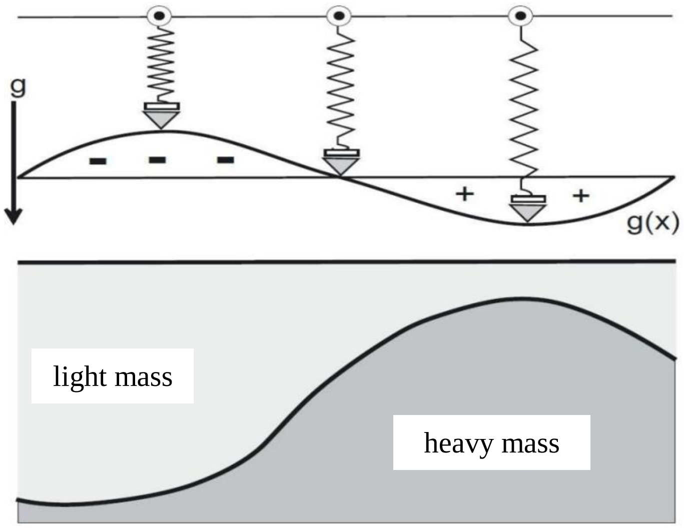

Figure 2. 1 Subsurface heterogeneities are sources of gravity variations (Dubois and Diament, 2011).

II.3. Newton's Law of Gravitation

In 1687, Isaac Newton established that every two masses in the universe attract each other with a force that is proportional to the product of their masses and inversely proportional to the square of the distance separating them. This gravitational force F between two masses, M and mmm, separated by a distance ddd, is expressed as:

$$F = G\frac{M \cdot m}{d^2}$$

where:

- F is the gravitational force (in newtons, N),

- M and m are the two masses (in kilograms, kg),
- d is the distance between the centers of the two masses (in meters, m),
- G is the universal gravitational constant, with a value of approximately $6.674\times10^{-11}\ m^3kg^{-1}s^{-2}$.

This fundamental law underpins gravimetry, as variations in the Earth's gravitational field arise from differences in subsurface mass distributions, which generate measurable gravitational forces detectable at the surface.

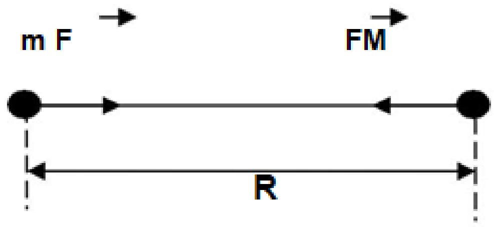

Figure 2. 2 Mutual gravitational attraction between two masses.

II.4.Newton’s Second Law and Gravitational Acceleration

A force F must be applied to a mass m to produce an acceleration a (Halliday *et al.*, 2013, Lowrie & Fichtner, 2020). This relationship is expressed as:

$$F = m \times a$$

When considering the gravitational force acting on a mass mmm at the Earth’s surface, we have:

$$F = \frac{GM}{R^2} = g_n m$$

where:

- M is the mass of the Earth,
- R is the mean radius of the Earth ($R\approx6370$ km),
- g_n is the acceleration due to gravity at the Earth’s surface, with an average value of approximately 9.81 m/s^2.

In honor of Galileo, the unit of gravitational acceleration was named the **gal**, defined as:

1 Gal=1 $cm/s^2=10^{-2}\ m/s^2$

Other related units include:

- 1 mGal=10^{-3} Gal
- The modern SI unit **gu (gravity unit)**: 1 gu=$10^{-6}\ m/s^2$=0.1 mGal

Using these relationships, the acceleration of a mass m on the Earth's surface can be expressed as:

$$g = \frac{GM_T}{R_T^2} \approx 9.81\,\mathrm{m/s^2}$$

where MT=5.9736×1024 kg is the Earth's mass and RT=6370 km is the mean Earth radius. The quantity g is commonly called the acceleration of gravity or simply gravity, and its average value at the Earth's surface is approximately 9.797 m/s2.

II.5. The Gravimetric Field

The Earth's gravitational field is not constant but varies under the influence of several factors (Telford *et al.*, 1990, Stacey & Davis, 2008):

- **Latitude** affects gravity because of the Earth's oblate spheroid shape and rotation, producing higher values at the poles (≈9.83 m/s^2) and lower values at the equator (≈9.78 m/s^2).
- **Altitude** also modifies gravity, with acceleration decreasing as elevation increases, approximately by **0.3086 mGal per meter** above sea level.
- Local **topography** plays a significant role: mountain masses increase the gravitational field, while valleys and basins reduce it, requiring terrain corrections in gravimetric surveys.
- **Earth tides** caused by the gravitational attraction of the Moon and Sun lead to periodic variations of up to several hundred microgals in surface gravity.
- **Subsurface density variations** create local gravity anomalies, with dense bodies such as mafic intrusions or ore deposits generating positive anomalies, while low-density features like sedimentary basins or salt domes yield negative anomalies. Together, these factors explain why precise gravity measurements must account for both global and local influences

II.6. Earth's Gravity

To predict the Earth's gravitational field at any location, it is necessary to know both its shape and the variations in its internal density. The Earth is not a perfect sphere but an **oblate spheroid**, flattened at the poles and bulging at the equator, which causes systematic variations in gravitational acceleration with latitude. In addition, the planet's interior is compositionally heterogeneous, with density contrasts between the crust, mantle, and core, as well as local variations caused by geological structures such as sedimentary basins, magmatic intrusions, or mountain roots. These density variations produce **gravity anomalies**, which are measurable deviations from the theoretical gravitational field of a homogeneous ellipsoid. Accurate prediction of Earth's gravity field therefore requires models that integrate both the **geometric shape of the geoid** and the **distribution of mass within the Earth** (Telford *et al.*, 1990, Lowrie & Fichtner, 2020, Stacey & Davis, 2008).

The gravity calculated for this spheroidal Earth represents the **theoretical or normal gravity** at sea level, defined on a reference body whose shape closely approximates the actual Earth. This reference model assumes that density varies only with depth and not laterally, meaning that local geological heterogeneities are ignored. The **equation for normal (theoretical) gravity** (the *International Gravity Formula*) is not the work of a single author. It was developed and adopted by international geodetic organizations, based on measurements and adjustments over many years.

- The **original form** of the normal gravity formula comes from the **International Union of Geodesy and Geophysics (IUGG)**.
- The most widely used modern version is the **1967 International Gravity Formula (IGF67)**, later refined in **1980** (WGS-84 reference ellipsoid).

$$g(\varphi) = 9.780327\left(1 + 0{,}0053024\, sin^2(\varphi) - 0.0000058\ sin^2(2\varphi)\right) \quad (\frac{m}{s^2})$$

This **International Gravity Formula (1967)** was adopted by the IUGG and is cited in most geophysics/geodesy textbooks (e.g., Telford et al., 1990; Lowrie, 2007).

Newton's laws provide the gravitational acceleration g_N. However, due to the Earth's rotation, a centrifugal force arises, introducing an additional component g_c. Therefore, the gravity measured at the Earth's surface, g, is the sum of the Newtonian gravitational component and the centrifugal component:

$$g = g_N + g_c$$

(Laurent, 2009). This total gravity forms the basis for identifying anomalies caused by subsurface density contrasts.

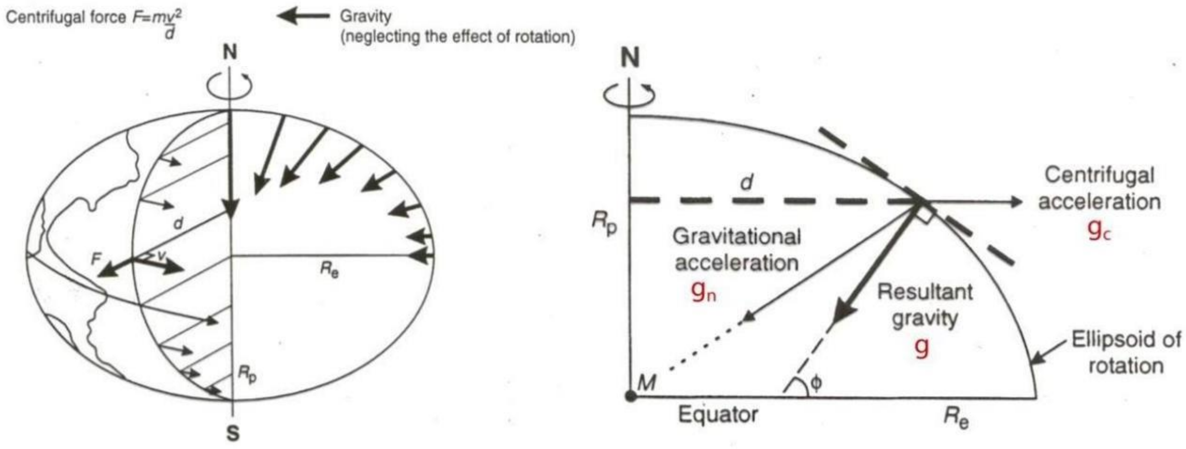

Figure 2. 3 Centripetal and centrifugal accelerations acting on the Earth's surface (Laurent, 2009).

II.7. Reference Geoid and Ellipsoid

- **Geoid:** The geoid is an equipotential surface of the Earth's gravitational field that coincides, on average, with the level of the oceans at rest and extends beneath the continents' topography. It serves as the reference surface for altitudes (level 0) and defines the true shape of the Earth (Dubois and Diament, 2011).
- **Reference Ellipsoid:** The reference ellipsoid is an ellipsoid of revolution that provides the best mathematical approximation of the geoid. It corresponds to an equipotential surface of the theoretical gravitational field of the Earth and is commonly used in geodetic and gravimetric calculations (Dubois and Diament, 2011).

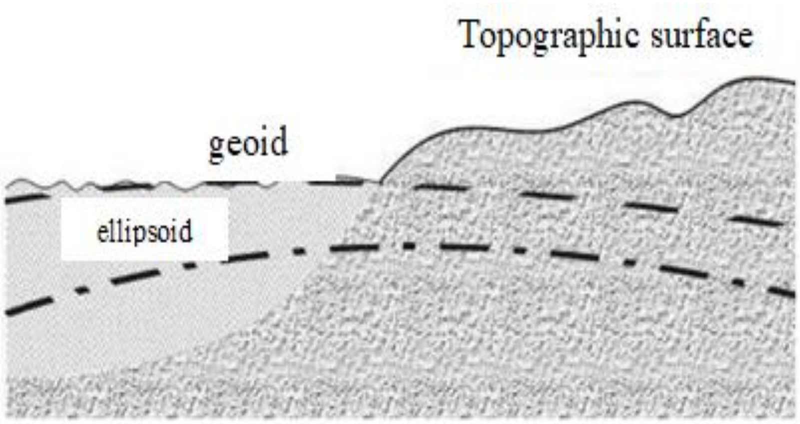

Figure 2. 4 The geoid is an equipotential surface of the Earth's gravitational field (Dubois and Diament, 2011).

II.8. Measuring Gravity: The Gravimeter

There are absolute gravimeters, which measure the total gravitational field “g”. These absolute gravimeters are not commonly used in gravimetric prospecting because they are too large and complex to operate.

Instead, relative gravimeters are used. They measure only the relative variations of the gravitational field.

A relative gravimeter can be represented by a spring holding a mass. A slight change in the gravitational attraction g causes the mass to move, leading to a small change in the length x of the spring.

To measure “g” with a precision of 0.01 mGal, the relative variation of the spring length ($\Delta x/x$) must be determined with an accuracy of one part in 10^8, which is extremely precise. Gravimeters are therefore complex and expensive instruments.

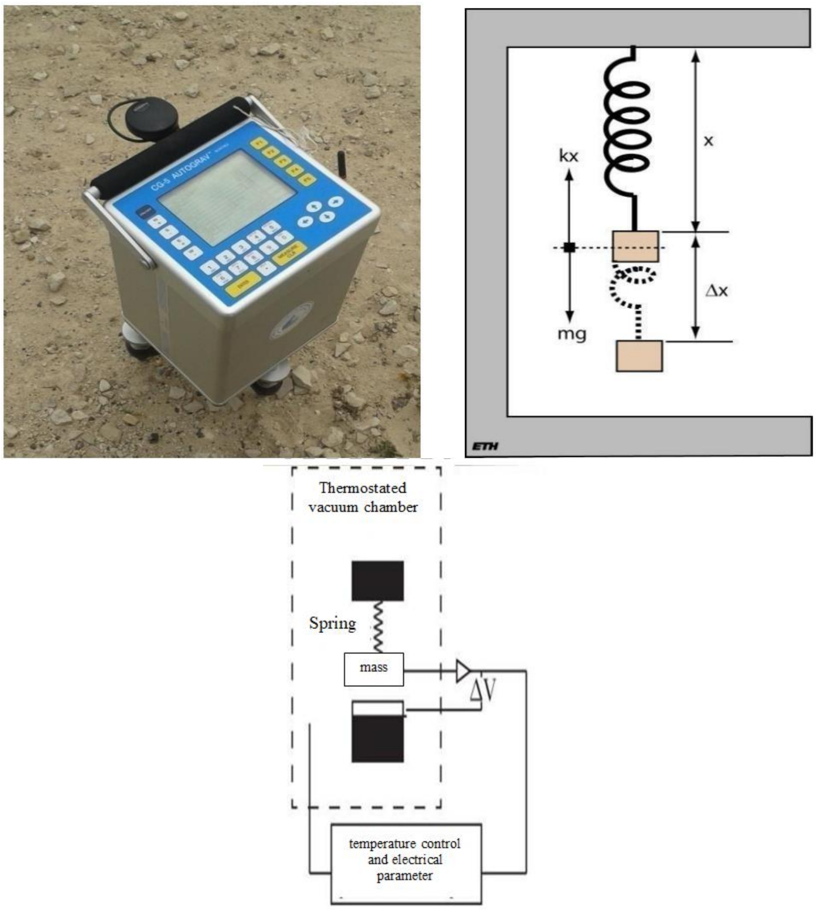

Figure 2. 5 Scintrex CG-5 relative gravimeter and its operating diagram (Dubois and Diament, 2011).

Modern instruments (such as the **CG5 Autograv from Scintrex**) can automatically level themselves (the gravimeter must be placed on a horizontal surface) and measure gravity by performing repeated measurements to enhance data quality (up to 6 measurements per second). Inconsistent noise is attenuated by filtering this data.

These instruments use a more advanced system than the simple spring mechanism described previously to measure gravity.

A variation in subsurface density results in a change in the gravitational attraction:

- **Mass deficit:** indicates the presence of a cavity, less dense ground, or zones of decompression.
- **Mass surplus:** indicates geological variations such as changes in the bedrock roof or the presence of denser materials.

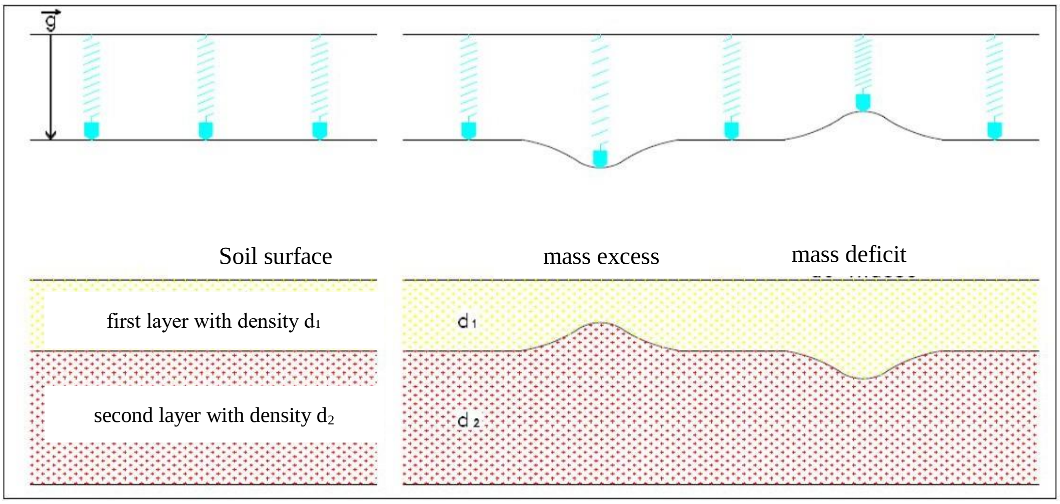

Figure 2. 6 Subsurface heterogeneities as sources of gravity variations

II.9. Microgravimetry

Microgravimetry is a gravimetric technique applied at the **local scale**, where the objective is to detect very small variations in the gravitational field, generally **less than 0.1 mGal (100 µGal)**. Such precision makes it possible to investigate fine subsurface structures that are not detectable with conventional gravimetric surveys.

This method is used in a wide range of applications, such as:

- **Engineering geology:** detection of cavities, sinkholes, or subsidence zones.
- **Archaeology:** identification of buried structures or voids.
- **Environmental studies:** mapping of waste deposits or landfills.
- **Volcanology and tectonics:** monitoring density changes related to magma movement or fault activity.

II.10. Principle and Measurement

- Measurements are performed with **highly sensitive relative gravimeters**, capable of detecting variations on the order of a few µGal.

- Station spacing is typically **metric (a few meters apart)**, in contrast to regional gravimetric surveys where spacing may reach hundreds of meters or kilometers.

- The method requires **precise elevation control**, because even small changes in altitude strongly influence gravity readings. This is generally achieved using **high-precision GPS** or **geometric leveling**.

II.11. Correction for Height Variations

A crucial aspect of micro-gravimetry is accounting for vertical position:

- A vertical displacement of only **10 cm** corresponds to a change of about **0.03 mGal** in the measured gravity.

- Therefore, elevation errors directly introduce false gravity anomalies, which can mislead interpretation if not properly corrected.

<u>Interpretation</u>

- **Mass deficit (negative anomaly):** indicates the presence of cavities, porous zones, decompressed terrains, or less dense materials.

- **Excess mass (positive anomaly):** reflects denser bodies such as intrusions, uplifted bedrock, or compacted zones.

Thus, microgravimetry provides a powerful tool for **high-resolution imaging of near-surface density variations**, bridging the gap between regional gravimetric methods and direct geotechnical investigations.

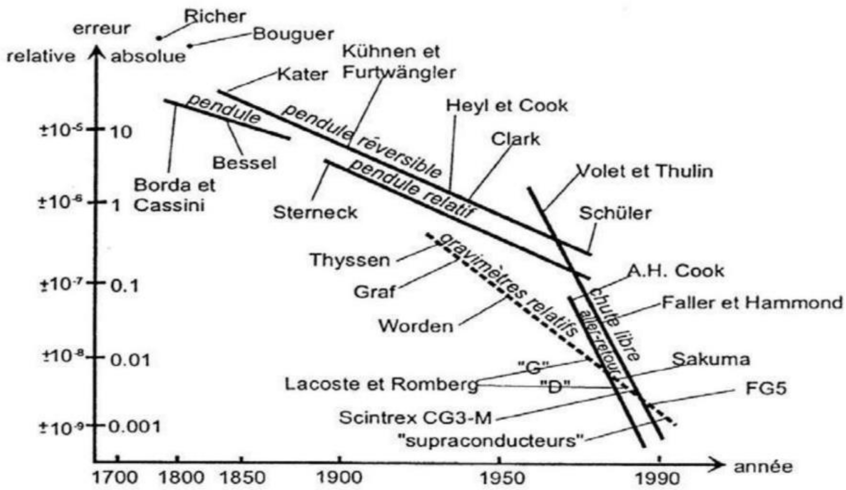

Figure 2. 7 Evolution of the accuracy of absolute and relative gravimeters (after Torge, modified by S. Merlet). The absolute error is expressed in mGal (Dubois and Diament, 2011).

II.12. Gravimetric Prospecting

In gravimetric prospecting, a relative gravimeter is used to measure relative variations in gravity between different stations, arranged either along a profile or within a survey grid on the ground.

Precise positioning of each measurement station is essential:

- Horizontal accuracy must be within a few centimeters.
- Vertical accuracy must be better than one centimeter.

To achieve this, differential GPS techniques are commonly employed.

At each station, several repeated readings are taken during a gravimetric measurement cycle (see figure below). The stations are then tied to a gravimetric base station, where the absolute value of gravity is already known. Such networks of base stations exist, for example, in Tunisia.

From this process, the measured or observed gravity data (g_obs) are obtained.

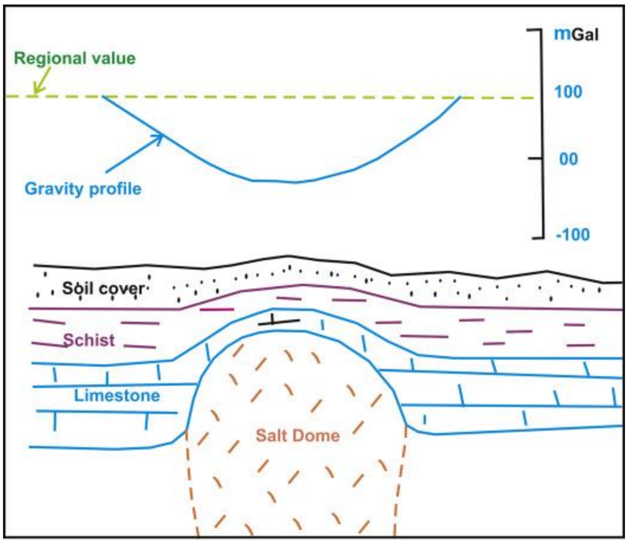

Figure 2. 8 Principle of gravimetric data acquisition.

II.13. Corrections in Gravimetric Prospecting

When performing gravimetric surveys, the raw measurement given by the gravimeter must be corrected to eliminate effects unrelated to subsurface density contrasts. The corrected value is called the **Bouguer anomaly**.

a) Instrumental Drift Correction

Gravimeters are very sensitive and may “drift” with time.

- To correct this, gravity is remeasured at a base station before and after the survey.
- The difference is distributed linearly over the survey time and subtracted from the data.

$$g_{corr} = g_{obs} - g_{drift}$$

b) Tidal Correction

The Moon and Sun cause small periodic variations in gravity.

- These are predicted from astronomical tables and subtracted from the observations.

$$g_{corr} = g_{obs} - g_{tida}$$

c) Latitude Correction (Normal Gravity)

Gravity varies with latitude because of Earth's rotation and flattening.

- The theoretical value of gravity at sea level and latitude φ\varphiφ is given by the **International Gravity Formula (IGF 1980):**

$$g_0(\varphi) = 978032.7(1 + 0.0053024(\sin\varphi)^2 - 0.0000058(\sin 2\varphi)^2)mGal$$

Measured values are corrected to this reference.

d) Free-Air Correction (FAC)

Gravity decreases with altitude above sea level because of increased distance from Earth's center.

- The correction adds back this effect:

$$\Delta g_{FA} = +0{,}3086h \quad (mGal)$$

where h is the station elevation in meters.

e) Bouguer Correction

The rock slab between the station and sea level adds extra attraction.

- The Bouguer correction removes this effect:

$$\Delta g_b = -0{,}0419\rho h\ (mGal)$$

where:

- ρ = average rock density (g/cm³)
- h = elevation (m)

6. Terrain Correction

Local relief (hills, valleys) around the station modifies gravity.

- Terrain correction removes this local effect using topographic maps or digital elevation models.

Final Bouguer Anomaly

After applying all corrections, the **Bouguer anomaly** is:

$$\Delta g_{Bouguer} = g_{obs} + \Delta g_{FA} + \Delta g_B + \Delta g_{Terrain} - g_0(\varphi) - g_{tidal} - g_{drift}$$

This anomaly reflects **only subsurface density contrasts** and is used for geological interpretation.

Exercise 1 — Full Bouguer anomaly (worked example)

Given: station at latitude $\varphi = 35^\circ$, elevation $h = 500$ m, rock density $\rho = 2.67\ \mathrm{g} \backslash \mathrm{cm}^{3}$.
Measured gravity (observed): $g_{obs} = 979635.0000$ mGal.
Assume no tidal or drift corrections and no terrain correction ($g_{tidal} = g_{drift} = \Delta g_{terrain} = 0$).
Compute the **Bouguer anomaly.**

Formulas used

1. Normal gravity (IGF 1980):

$$g_0(\varphi) = 978032.7\left(1 + 0.0053024 \sin^2 \varphi - 0.0000058 \sin^2 2\varphi\right)\ (\mathrm{mGal})$$

2. Free-air correction:

$$\Delta g_{FA} = +0.3086\, h\ (\mathrm{mGal})$$

3. Simple Bouguer slab correction:

$$\Delta g_B = -0.0419\, \rho\, h\ (\mathrm{mGal})$$

4. Final Bouguer anomaly:

$$\Delta g_{Bouguer} = g_{obs} + \Delta g_{FA} + \Delta g_B + \Delta g_{terrain} - g_0(\varphi) - g_{tidal} - g_{drift}$$

Solution (step by step)

1. Compute $\sin(35^\circ)$ and $\sin(70^\circ)$ (values kept to sufficient precision for students):
$\sin 35^\circ \approx 0.573576 \rightarrow \sin^2 35^\circ \approx 0.328989$.
$\sin 2\varphi = \sin 70^\circ \approx 0.939693 \rightarrow \sin^2 2\varphi \approx 0.883022$.
2. Compute the bracket in IGF:

$$1 + 0.0053024(0.328989) - 0.0000058(0.883022)$$

Compute each term:

- $0.0053024 \times 0.328989 \approx 0.001743945$
- $0.0000058 \times 0.883022 \approx 0.000005121$

Thus bracket ≈ 1.001738824.

3. Normal gravity:

$$g_0(35^\circ) = 978032.7 \times 1.001738824 \approx 979733.33\ \mathrm{mGal}$$

(rounded to two decimals: **979733.33 mGal**).

4. Free-air correction:

$$\Delta g_{FA} = 0.3086 \times 500 = 154.30\ \mathrm{mGal}$$

5. Bouguer slab correction:

$$\Delta g_B = -0.0419 \times 2.67 \times 500 = -55.9365\ \mathrm{mGal}$$

6. Insert into final formula (terrain, tidal, drift = 0):

$$\Delta g_{Bouguer} = 979635.0000 + 154.3000 - 55.9365 - 979733.33$$

Compute numerator:

- $979635.0000 + 154.3000 = 979789.3000$
- $979789.3000 - 55.9365 = 979733.3635$

Then

$$\Delta g_{Bouguer} = 979733.3635 - 979733.33 = \boxed{+0.03\ \mathrm{mGal}}\ (\approx +0.0335\ \mathrm{mGal})$$

Answer: Bouguer anomaly ≈ **+0.03 mGal** (small positive anomaly in this hypothetical example).

Chapter.3 Electrical methods

III.1. Introduction

Commonly used electrical methods in applied geophysics comprise direct-current (DC) electrical measurements, self-potential measurements (SP) and induced-polarisation methods (IP), including spectral-induced polarisation (SIP).

The SP method is based on passive measurements of natural electrical potential differences in the ground, which are often negligible in periglacial areas as electrically conductive materials or water flow have to be present to generate distinct SP patterns. A cryospheric example measuring subglacial drainage conditions with SP is given by Kulessa et al. (2003).

The IP and SIP methods are based on actively induced polarisation effects in the subsurface, which require polarisable material to be present. Again, these effects are usually small in frozen environments, which is why all three methods have seldom been used in periglacial research to date. A review concerning SP and IP methods is included in the review paper concerning the application of geophysical methods in permafrost areas by Scott et al. (1990). Further details on these techniques are given in Weller and Bo¨rner (1996) and Slater and Lesmes (2002).

III.2. Measurement principles

Resistivity surveys are conducted by injecting a direct electrical current (I) into the ground via two current electrodes (A and B in Figure 1.1). The resulting voltage difference (DV) is measured at two potential electrodes (M and N). The overall purpose of resistivity measurements is to determine the subsurface resistivity distribution. From the current (I) and voltage difference values (DV) the resistivity q is calculated using

$$\rho_a = K\frac{DV}{I}$$

where K is a geometric factor that depends on the arrangement of the four electrodes. This calculated resistivity value is not the ‘true’ resistivity of the subsurface, but a so-called ‘apparent resistivity’ qa, which equals the ‘true’ (or specific) resistivity only for a homogeneous subsurface. For heterogeneous resistivity distributions in the ground the resistivity can be derived from the measured apparent resistivity values using inversion methods implemented, for instance, in commercially available software programmes. The basic principle for the successful application of geoelectrical methods in geomorphology/quaternary geology is based on the varying electrical conducti- vity (= 1/resistivity) of minerals, solid bedrock, sediments, air and water, and consequently their varying electrical resistivity (Table 1.1). Resistivity surveys give an image of the subsurface resistivity distribution. Knowing the resistivities of different material types, it is possible to convert the resistivity image into an image of the subsurface consisting of different materials. However, as a conse- quence of overlapping resistivity values of different materials, this conversion might be non-unique.

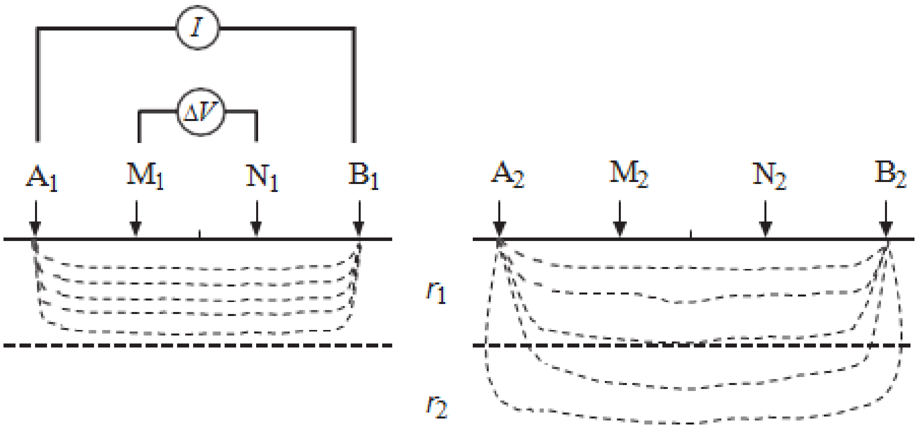

Figure 3. 1 Conventional four-electrode configuration in resistivity surveys.

Table 3 Range of resistivities for different materials (Kneisel (1999)

Material	Range of resistivity (W m)
Clay	1–100
Sand	$100–5 \cdot 10^3$
Gravel	$100–4 \cdot 10^2$
Granite	$5 \cdot 10^3–10^6$
Gneiss	$100–10^3$
Schist	$100–10^4$
Groundwater	10–300
Frozen sediments,	$1 \cdot 10^3–10^6$
ground ice, mountain permafrost^d Glacier ice (temperate)	$10^6–10^8$
Air	infinity

When the distance between the current electrodes (A, B) is increased, a larger penetration depth is obtained (as indicated in Figure 3.1) yielding more infor- mation about the deeper sections of the subsurface. The penetration depth d depends on the measurement geometry and is limited by the maximum electrode spacing. It may be estimated using a formula by Barker (1989) with d = 0.17L for the so-called Wenner array (see below), with L being the distance between the outer (current) electrodes.

III.3. Measurement configuration and array types

III.3.1. Vertical electrical soundings (VES)

For electrical resistivity surveys different array types are used. In traditional one-dimensional DC resistivity soundings (or vertical electrical soundings, VES) the symmetrical Schlumberger array is applied. In Schlumberger surveys the distance between the outer current electrodes is increased logarithmically to obtain a sounding curve with maximum penetration depth, while the distance between the potential electrodes remains mostly constant. For the interpretation of one-dimensional data the assumption is made that the subsurface consists of horizontal layers and that the resistivity changes only with depth but not horizontally. The obtained resistivity values are interpreted as a one- dimensional layered model of the subsurface using standard software packages.

III.3.2. Wenner profiling

The resistivity profiling method is used for obtaining lateral changes in the subsurface resistivity. In this case, the Wenner array is applied where the spacing between the electrodes remains fixed, but all four electrodes are moved simultaneously for each reading. Wenner profiling is used to obtain information about lateral changes, but not about vertical changes in resistivity.

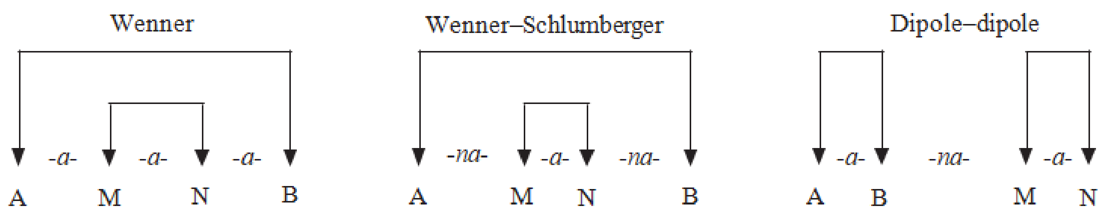

Figure 3. 2 Schematics of the most commonly used array geometries in ERT surveys.

III.4. Electrical resistivity tomography (ERT)

From the description above, the limitations of Schlumberger sounding and Wenner profiling surveys are evident. The assumed horizontal layering as well as the assumption that resistivity changes only with depth but not horizontally will not always be valid in practice. On heterogeneous ground conditions, the interpretation of one-dimensional soundings can be difficult, as lateral variations along the survey line can influence the results significantly. The sounding curve produces an average resistivity model of the survey area. For some studies this might not be problematic and the results obtained from one-dimensional soundings are sufficient. However, individual anomalies will not show explicitly in the results. Two-dimensional resistivity tomography (ERT) overcomes this problem using multi-electrode systems and two-dimensional data inversion yielding a more accurate model of the subsurface (see Chapters 6, 8, 9 and 10). ERT requires multiple resistivity measurements with various electrode spacings along a profile line (2D) or on a two-dimensional grid (3D). The most commonly used measurement geometries in ERT surveys are the Wenner, Wenner– Schlumberger and Dipole–dipole arrays (see Figure 3.2).

III.5. Data acquisition

Compared to vertical electrical soundings, which typically involve 10 to 20 readings, ERT imaging surveys consist of 100 to several hundred measurements. Depending on the quality of the recorded voltages, the measurements for each electrode configuration have to be repeated until the variance is less than a pre-defined threshold. Acquiring a full ERT data set with about 40 electrodes requires between 0.5 and 1.5 hours (depending on the configuration). The time for data acquisition depends on the number of measured electrode combinations (often called quadripoles) and on the number of repetitions of a single combination.

For the acquisition of the apparent resistivity data sets, multi-electrode systems are commonly used. These systems automatically measure the apparent resistivity's for a series of electrode combinations for a given array geometry. Using 40 equally spaced electrodes with a spacing of 5 m and a Wenner array results in a data set of 190 apparent resistivities, a survey line of 195 m length and a penetration depth of about 30 m.

Choice of an appropriate electrode configuration is dependent on the difficult surface conditions associated with mountain regions. Since the maximum current injected into the ground can be quite low, the geometrical factors of the electrode configurations may be critical (Telford *et al.* 1990). For this reason, often Wenner or Wenner–Schlumberger configurations are employed, even though Dipole–dipole configurations may provide superior lateral resolution (Loke 2004).

Further details on different array geometries are given, for instance, in Telford *et al.* (1990) and Reynolds (1997). Applications of different arrays to various geomorphological studies are described in Kneisel (2003, 2006).

III.6. Data processing

Data processing consists basically of applying an appropriate inversion algorithm to the observed apparent resistivity data set to determine the specific resistivity values on a two-dimensional *x–z* model grid. During the past few years, two- and three-dimensional inversion algorithms for resistivity data have been developed and applied successfully in many environmental and archaeological applications (e.g. Johansson and Dahlin 1996, Mauriello *et al.* 1998, Ogilvy *et al.* 1999, Olayinka and Yaramanci 1999, Daily *et al.* 2004, Gu¨nther *et al.* 2006).

The development of **2D and 3D inversion software** such as *RES2DINV* and *RES3DINV* (Loke & Barker, 1995, 1996) greatly improved **Electrical Resistivity Tomography (ERT)**. Unlike pseudosections of apparent resistivity, inversion produces a **true resistivity model** of the subsurface, and can even include **topography**, which is important in mountainous terrains.

Before inversion, data must be checked and cleaned of **errors or abnormal values** (e.g., poor electrode contact). Two inversion approaches are available:

- **Least-squares (L2):** smooth models, but boundaries appear blurred.
- **Robust (L1):** better at preserving sharp geological contacts.

The process begins with a **homogeneous starting model** derived from average resistivity. The program then calculates synthetic resistivities and iteratively adjusts the model until it matches the measured data. The quality of the fit is evaluated with the **RMS error**.

Reliability is improved by testing different starting models (Marescot et al., 2003).

III.7. High Resistivity's and Large Resistivity Contrasts

In mountain environments, **ERT surveys** often show **very high resistivity values**, mainly due to the presence of **ground ice** (often of glacial origin). These values, however, can also be influenced by inversion parameters, survey geometry, or ambiguities such as the **principle of equivalence** (Telford et al., 1990).

A key application has been the **detection of ground ice in rock glaciers and ice-cored moraines**. Research usually focuses on:

1. The **occurrence and extent** of ground ice,
2. The **ice content**,
3. The **origin of the ice**.

Field examples:

- **Rock glacier Murtel (Swiss Alps):**

    - Maximum resistivities up to **2 MΩ·m** between 5–15 m depth, matching massive ice observed in a borehole.
    - Resistivities decrease at depth due to increasing debris content.
    - Sharp resistivity gradient marks the glacier tongue.
    - Non-permafrost areas show resistivities < **5 kΩ·m**.
- **Rock glacier Stelvio (Italian Alps):**
    - Resistivity maximum up to **500 kΩ·m**, thinner than at Murtel.
    - Sharp gradients at 10–25 m depth.
    - Different regions identified:
        - **A:** active, ice-rich (high resistivity),
        - **B:** less active/inactive (lower resistivity),
        - **C:** deeper low-resistivity zone, marking the lower boundary of ice-rich layers.

Interpretation:

- Very high resistivities (> 10^5 Ω·m) indicate frozen material.
- Sharp decreases in resistivity define the **horizontal and vertical extent of ice bodies**.
- At Murtel, resistivity results are confirmed by drill cores.
- At Stelvio, no boreholes exist, but geomorphology and vegetation analysis support the resistivity interpretation.

III.8. Electrode configuration and measurement geometry

The chosen electrode configuration can also influence the inversion results. Figure 3.3 shows results from measurements with both Wenner and Dipole–dipole arrays at a sporadic permafrost site in the Bever Valley, Swiss Alps. Areas with resistivity values as high as 120 kX m are interpreted as permafrost lenses, which are in good agreement with findings from vertical electrical soundings and refraction seismic tomography surveys (Kneisel *et al.* 2000, Kneisel and Hauck 2003).

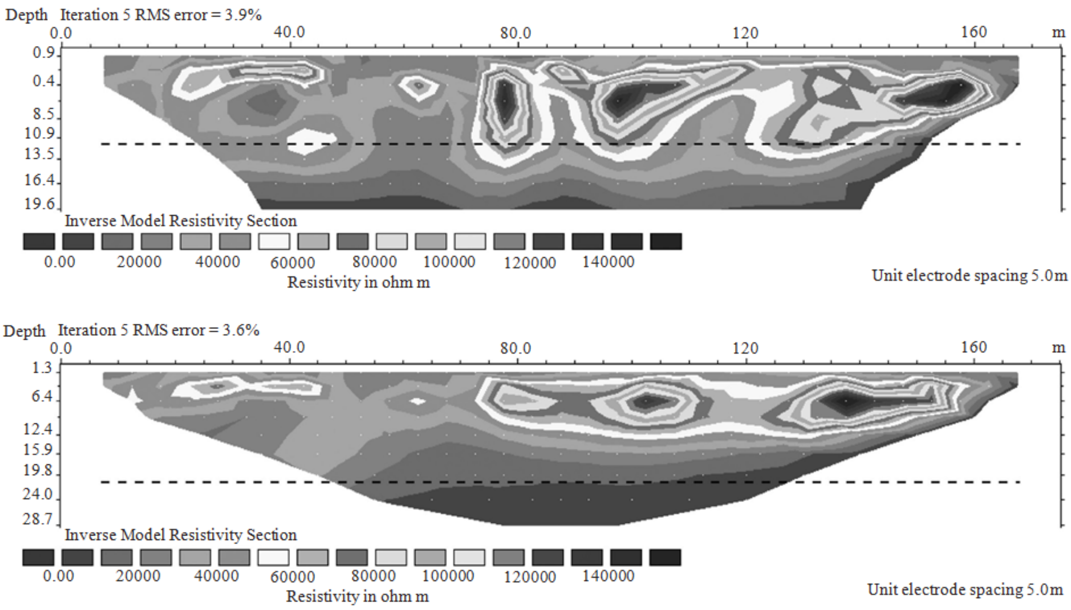

Figure 3. 3 Comparison of two resistivity tomograms performed at the same location: Dipole–dipole (upper panel) and Wenner survey (bottom panel) on a scree slope with isolated permafrost lenses. Electrode spacing is 5 m (permafrost study).

The choice of **array type** and **survey layout** plays a crucial role in Electrical Resistivity Tomography (ERT) surveys. A comparison of results shows that the **Dipole–dipole array** provides superior horizontal resolution but has a shallower penetration depth than the **Wenner array**. In many cases, Wenner data are sufficient for detecting the overall presence or absence of permafrost, while Dipole–dipole measurements are better suited for the detailed characterization of the location and extent of permafrost lenses. In addition to the array type, the **orientation of the survey line** can significantly influence the results, especially in areas with strong three-dimensional topographic variability. Hauck and Vonder Mühll (2003b) showed that resistivity values for an ice core were much higher (≈200 kΩ·m) for a longitudinal profile along the moraine top, compared with a cross-profile (≈110 kΩ·m). However, only the cross-profile allowed an estimation of the vertical extent of the ice body. Forward modelling also indicates that isolated anomalies tend to be underestimated in terms of absolute resistivity. These findings highlight that both **array geometry** and **profile orientation** must be carefully selected according to the specific aim of the survey.

III.9. Topography

Topographic corrections are especially important for regions with complex terrain, as the calculation of the electrical current density distribution of the subsurface is dependent on the surface topography (Tong and Yang 1990, Loke 2000, Gu¨nther *et al.* 2006). Figure 3.4 shows the resistivity inversion results of a 200 m long profile with (Figure 3.4a) and without (Figure 3.4b) topographic corrections during inversion.

This survey line was conducted over extreme altitudinal gradients including a downslope region (I in Figure 3.4) with an altitudinal difference of 50 m, a crossing of a small sediment-filled valley (region II), a 20 m altitudinal step to a flat rock plateau (region III) until it terminated on the eastern flank of the ice-cored moraine (region IV) discussed above. The different subsurface materials can easily be distinguished by their respective resistivity values (3–6 kX m: bedrock underneath the slope (I and II), 10–20 kX m: rock plateau (III) and >100 kX m: ice core (IV); Hauck and Vonder Mu¨hll 2003b).

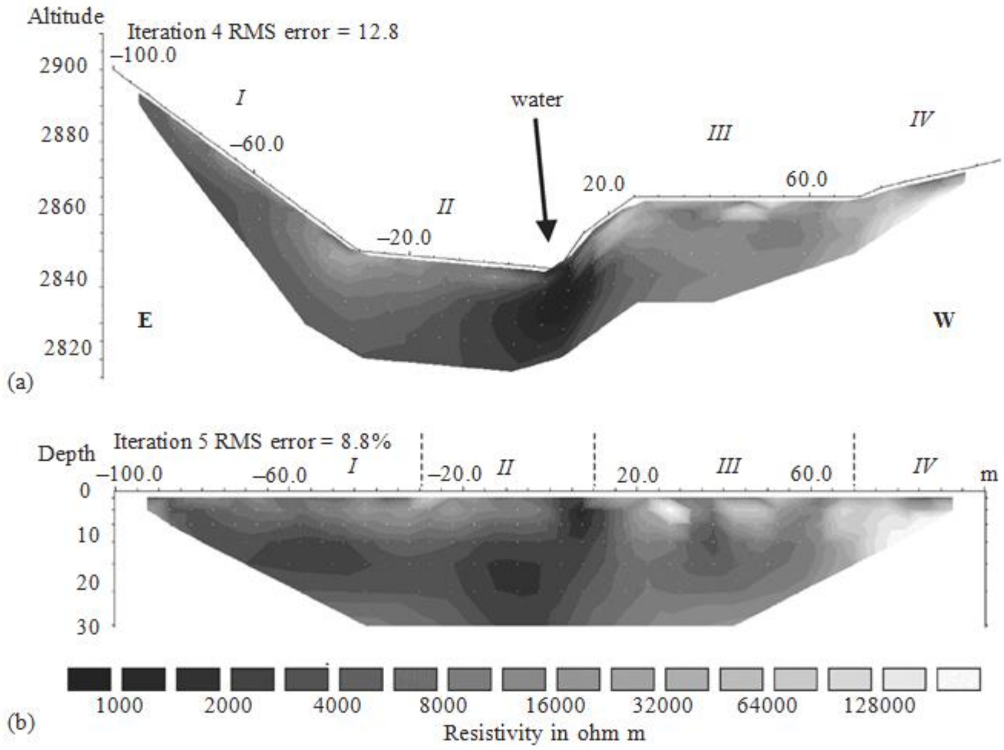

Figure 3. 4 Model inversion results for a survey line over complex geomor- phological terrain near Zermatt, Switzerland: (a) with and (b) without topographic corrections. Regions I–IV correspond to features explained in the text (from Hauck and Vonder Mu¨hll 2003b)

Comparing Figures 1.7a and 1.7b large differences can be found, especially in region III and near the surface water flow at horizontal distance 5 m. As can be seen from Figure 1.7b, an inversion without incorporated topography would yield erroneous results leading to possible misinterpretations of geological and peri- glacial features. For example, the low-resistivity zone at 10–20 m depth between horizontal distances –90 m and 60 m in Figure 1.7b could be misinterpreted as a permafrost-free layer, whereas these low resistivity values are solely due to inversion artefacts induced by the rather confined conductive zone of water flow seen in the vicinity of horizontal distance 5 m in Figure 1.7a. A large influence of topography on the inversion results is typical for complex terrain and heterogeneous subsurface characteristics.

III.10. Non-uniqueness of the interpretation of high resistivities due to air, ice, and bedrock

Although ERT is highly effective for detecting ground ice, thanks to the strong influence of unfrozen water and ice content on electrical resistivity, interpreting the results can be challenging in some permafrost environments. This difficulty arises because measured high resistivity values may result from different materials. While the resistivity contrast between ice and unfrozen water is very large, it can be quite small between ice, air, and certain rock types, since all three behave almost like electrical insulators (Table 3).

For this reason, ERT alone may not always provide clear results, and additional methods are often required to obtain unambiguous subsurface information. The most common complementary method is seismic refraction, as P-wave velocities differ greatly between ice (3500 m/s) and air (330 m/s). In later chapters (9 and 10), combined electrical and seismic datasets are used to quantify areas with high or low ice contents and to identify internal boundaries such as the base of the active layer more precisely. Other techniques are also frequently combined with ERT, including electromagnetic (EM) surveys, ground-penetrating radar (GPR), or multi-method approaches (e.g., Kneisel and Hauck 2003; Yoshikawa et al. 2006; Maurer and Hauck 2007).

III.11. Monitoring

Monitoring time-dependent processes (known as time-lapse experiments) involves repeating 2D resistivity surveys along the same profile at different times (e.g., Barker and Moore 1998; Hauck 2002; Hilbich et al. 2008). Achieving reliable results requires accurate and reproducible measurements, even on rough terrain. To minimize variations caused by changes in electrode positions or contacts, fixed-electrode arrays are often employed.

An example is Hauck (2002), who developed a semi-automated system on a mountain slope where fine-grained weathered material overlies bedrock. In this setup, a manual switchbox connected to permanently installed cables allowed year-round measurements, even under thick snow cover. A long-term ERT monitoring series from the Schilthorn (Swiss Alps), ongoing for seven years, demonstrates the effectiveness of this method on daily, seasonal, and interannual scales (Hilbich et al. 2008).

As an illustration, Figure 3.5 presents results from test measurements on a blocky moraine in the Muragl glacier forefield using a fixed array with 2 m electrode spacing. Despite the rough surface conditions, the inversion results proved reproducible and of good quality. Initially, the data were inverted independently. However, this approach provided only limited insight into temporal subsurface resistivity changes, since the inversion process tends to minimize the difference between measured and calculated apparent resistivity values.

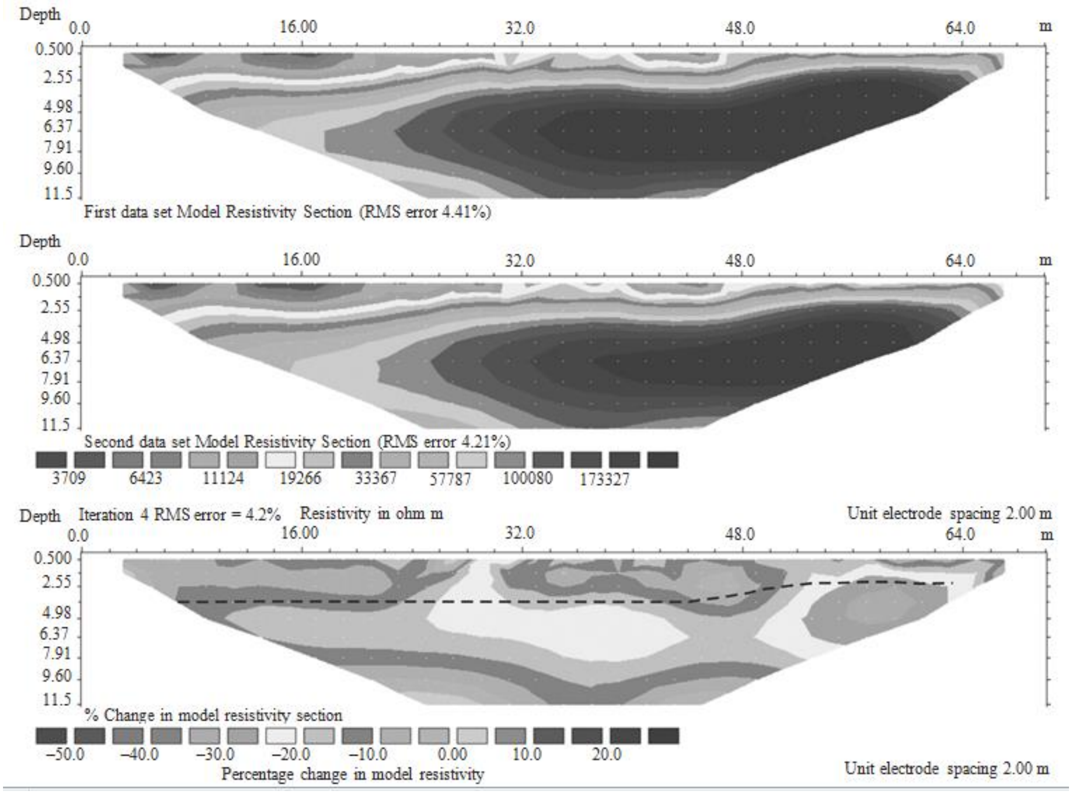

Figure 3. 5 Resistivity tomograms of a Wenner–Schlumberger survey on a moraine consisting partly of coarse debris. Upper panel represents the survey on 4 August, middle panel the survey on 27 August, bottom panel the percentage change in resistivity. Dashed line in

Chapter.4 Seismic methods

IV.1. Introduction

The seismic method exploits the variations in elastic wave propagation velocity within different geological media. This velocity is different for different rocks and it is this difference which is exploited in the seismic method. When we create sound at or near the surface of the earth, some energy will be reflected back (bounced back). They can be characterized as echoes. From these echoes we can determine the velocities of the rocks, as well as the depths where the echoes came from. In this chapter we will discuss the basic principles behind the behaviour of sound in solid materials. When we use the seismic method, we usually discuss two types of seismic methods, depending on whether the distance from the sound source to the detector (the ”ear”) is large or small with respect to the depth of interest: the first is known as refraction seismics, the other as reflection seismics. Of course, there is some overlap between those two types and that will be discussed in this chapter. When features really differ, then that will be discussed in next chapter for refraction and the chapters on reflection seismics. The overlap lies in the physics behind it, so we will deal with these in this chapter. In the following chapters will deal with instrumentation, field techniques, corrections (which are not necessary for refraction data) and interpretation.

IV.2. Basic physical notions of waves

Everybody knows what waves are when we are talking about waves at sea. Sound in materials has the same kind of behaviour as these waves, only they travel much faster than the waves we see at sea. Waves can occur in several ways. We will discuss two of them, namely the longitudinal and the shear waves. Longitudinal waves behave like waves in a large spring. When we push from one side of a spring, we will observe a wave going through the spring which characterizes itself by a thickening of the wires running through the spring in time (see also figure (2.1)). A property of this type of wave is that the motion of a piece of the wire is in the same direction as the wave moves. These waves are also called Push-waves, abbreviated to P-waves, or compressional waves. Another type of wave is the shear wave. A shear wave can be compared with a chord. When we push a chord upward from one side, a wave will run along the chord to the other side. The movement of the chord itself is only up- and downward: characteristic of this wave is that a piece of the chord is moving perpendicular to the direction of that of the wave (see also figure (2.1)). These types of waves are referred to as S-waves, also called dilatational waves. Characteristic of this wave is that a piece of the chord is pulling its ”neighbour” upward, and this can only occur when the material can support shear strain. In fluids, one can imagine that a ”neighbour” cannot be pulled upward simply because it is a fluid. Therefore, in fluids only P-waves exist, while in a solid both P- and S-waves exist. Waves are physical phenomena and thus have a relation to basic physical laws. The two laws which are applicable are the conservation of mass and Newton’s second law. These two have been used in appendix A to derive the two equations governing the wave motion due to a P-wave. There are some simplifying assumptions in the derivation, one of them being that we consider a 1-dimensional wave. When we denote p as the pressure and vx as the particle velocity, the conservation of mass leads to:

$$\frac{1}{K}\frac{\partial p}{\partial t} = -\frac{\partial v_x}{\partial x}$$

in which K is called the bulk modulus. The other relation follows from application of Newton's law:

$$-\frac{\partial p}{\partial x} = \rho\frac{\partial v_x}{\partial t}$$

where ρ denotes the mass density. This equation is called the equation of motion. The combination of these two equations leads, for constant density ρ, to the equation which describes the behavior of waves, namely the wave equation:

$$\frac{\partial^2 p}{\partial x^2} - \frac{1}{c^2}\frac{\partial^2 p}{\partial t^2} = 0$$

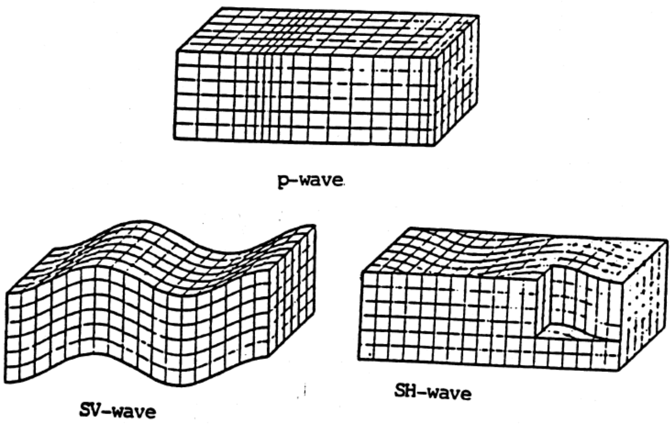

Figure 4. 1: Particle motion of P and S waves

in which c can be seen as the velocity of sound, for which we have: $c = \sqrt{\frac{K}{\rho}}$: The solution to this equation is:

$$p(x,t) = s(t \pm x/c)$$

where s(t) is some function. Note the dependency on space and time via $(t \pm x/c)$, which denotes that it is a travelling wave. The sign in the argument is depending on which direction the wave travelling in.

Often, seismic responses are analyzed in terms of frequencies, i.e., the Fourier spectra. The definition we use here is:

$$G(\omega) = \int_{-\infty}^{+\infty} g(t)\exp(-i\omega t)\,dt$$

we used the radial frequency ω instead: $\omega = 2\pi f$. Using this convention, it is easy to show that a differentiation with respect to time is equivalent to multiplication with iω in the Fourier domain. When we transform the solution of the wave equation (equation (2.4)) to the Fourier domain, we obtain:

$$P(x,\omega) = S(\omega)\exp(\pm i\omega x/c).$$

Note here that the time delay x/c (in the time domain) becomes a linear phase in the Fourier domain, i.e., $(\omega x/c)$. In the above, we gave an expression for the pressure, but one can also derive the equivalent expression for the particle velocity vx. To that purpose, we can use the equation of motion as expressed in equation (2.2), but then in its Fourier-transformed version, which is:

$$V_x(x,\omega) = -\frac{1}{i\omega\rho}\frac{\partial P(x,\omega)}{\partial x}.$$

When we substitute the solution for the pressure from above (equation (2.6)), we get for the negative sign:

$$\begin{aligned} V_x(x,\omega) &= -\frac{1}{i\omega\rho}S(\omega)\frac{-i\omega}{c}\exp(-i\omega x/c) \\ &= S(\omega)\frac{1}{\rho c}\exp(-i\omega x/c). \end{aligned}$$

Notice that the particle velocity is a scaled version of the pressure:

$$V_x(x,\omega) = \frac{P(x,\omega)}{\rho c}.$$

The scaling factor is (ρc), being called the seismic impedance.

Table 4 Seismic wave velocities for common materials and rocks(P-wave)

Material	velocity (m/s)	Material	velocity (m/s)
Air	330	Sandstone	2000-4500
Water	1500	Shales	3900-5500
Soil	20-300	Limestone	3400-7000
Sands	600-1850	Granite	4800-6000
Clays	1100-2500	Ultra-mafic rocks	7500-8500

.

IV.3. Types of Seismic Waves

There are several different kinds of seismic waves, and they all move in different ways. The two main types of waves are body waves and surface waves. Body waves can travel through the earth's inner layers, but surface waves can only move along the surface of the planet like ripples on water. Earthquakes radiate seismic energy as both body and surface waves.

IV.3.1. P WAVES

The first kind of body wave is the P wave or primary wave. This is the fastest kind of seismic wave, and, consequently, the first to 'arrive' at a seismic station. The P wave can move through solid rock and fluids, like water or the liquid layers of the earth. It pushes and pulls the rock it moves through just like sound waves push and pull the air. Have you ever heard a big clap of thunder and heard the windows rattle at the same time? The windows rattle because the sound waves were pushing and pulling on the window glass much like P waves push and pull on rock. Sometimes animals can hear the P waves of an earthquake. Dogs, for instance, commonly begin barking hysterically just before an earthquake 'hits' (or more specifically, before the surface waves arrive). Usually people can only feel the bump and rattle of these waves. P waves are also known as compressional waves, because of the pushing and pulling they do. Subjected to a P wave, particles move in the same direction that the the wave is moving in, which is the direction that the energy is traveling in, and is sometimes called the 'direction of wave propagation.

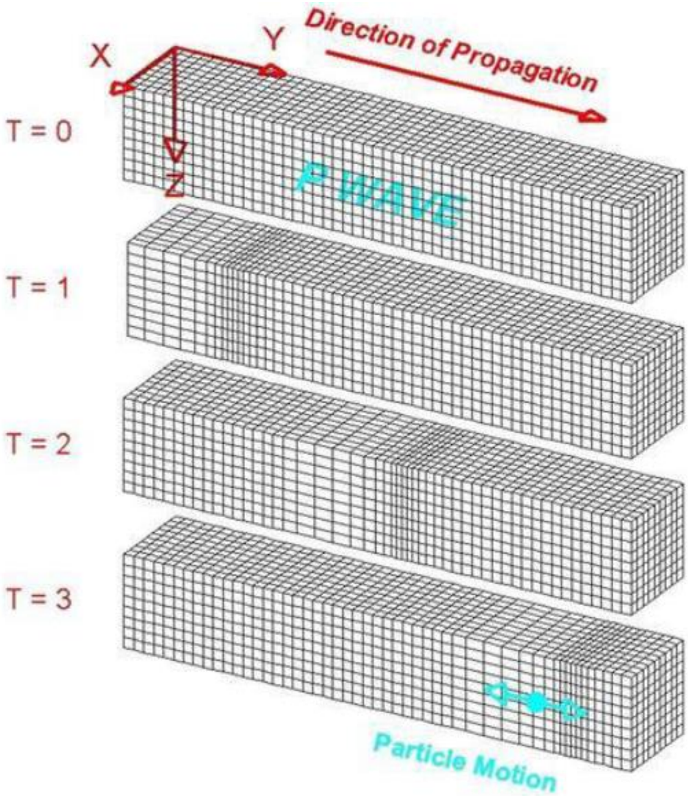

Figure 4. 2: Wave travels through a medium by means of compression and dilation. Particles are represented by cubes in this model.

IV.3.2. S WAVES

The second type of body wave is the S wave or secondary wave, which is the second wave you feel in an earthquake. An S wave is slower than a P wave and can only move through solid rock, not through any liquid medium. It is this property of S waves that led seismologists to conclude that the Earth's outer core is a liquid. S waves move rock particles up and down, or side-to-side--perpendicular to the direction that the wave is traveling in (the direction of wave propagation).

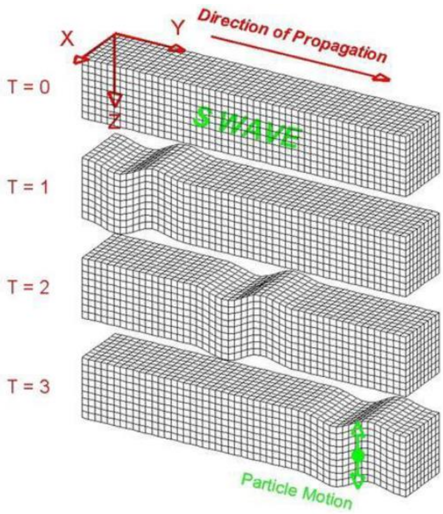

Figure 4. 3: An s wave travels through a medium. Particles are represented by cubes in this model.

IV.3.3. SURFACE WAVES

Travelling only through the crust, surface waves are of a lower frequency than body waves, and are easily distinguished on a seismogram as a result. Though they arrive after body waves, it is surface waves that are almost entirely responsible for the damage and destruction associated with earthquakes. This damage and the strength of the surface waves are reduced in deeper earthquakes.

a) LOVE WAVES

The first kind of surface wave is called a Love wave, named after A.E.H. Love, a British mathematician who worked out the mathematical model for this kind of wave in 1911. It's the fastest surface wave and moves the ground from side-to-side. Confined to the surface of the crust, Love waves produce entirely horizontal motion.

b) RAYLEIGH WAVES

The other kind of surface wave is the Rayleigh wave, named for John William Strutt, Lord Rayleigh, who mathematically predicted the existence of this kind of wave in 1885. A Rayleigh wave rolls along the ground just like a wave rolls across a lake or an ocean. Because it rolls, it moves the ground up and down, and side-to-side in the same direction that the wave is moving. Most of the shaking felt from an earthquake is due to the Rayleigh wave, which can be much larger than the other waves.

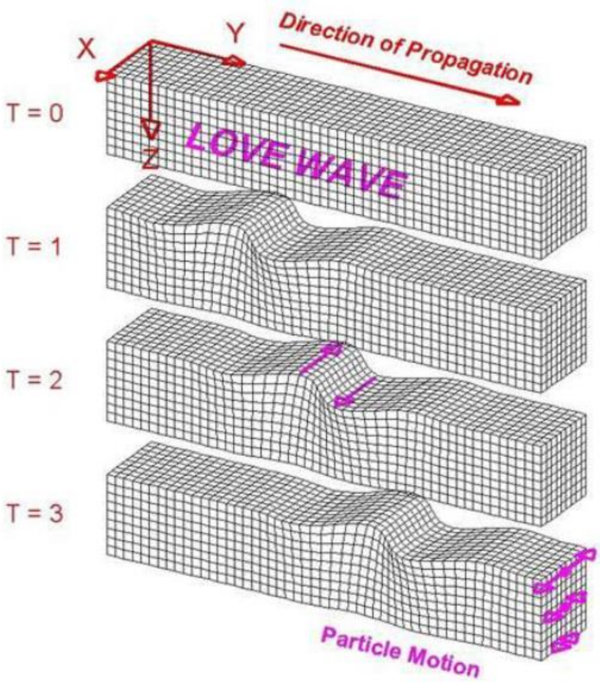

Figure 4. 4: A love wave travels through a medium. Particles are represented by cubes in this model.

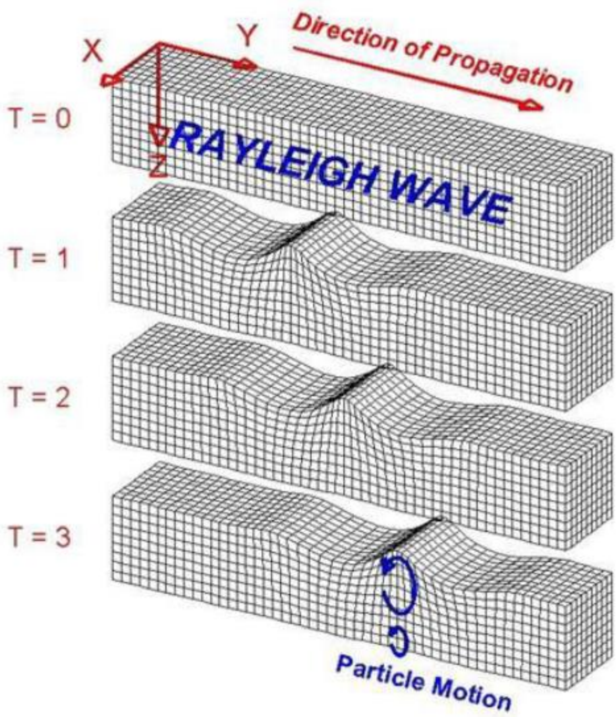

Figure 4. 5: A rayleigh wave travels through a medium. Particles are represented by cubes in this model.

IV.4. Seismic Prospecting

Seismic prospecting relies on measuring the travel time of compression waves (also known as longitudinal waves). The velocity of a medium is closely related to the characteristics of the material it passes through, such as density, hardness, porosity, and compaction. This method therefore makes use of wave propagation along geological interfaces to estimate a velocity model and the dip of the layers. Several types of waves are recorded by this technique, as illustrated in the following two-layer tabular example.

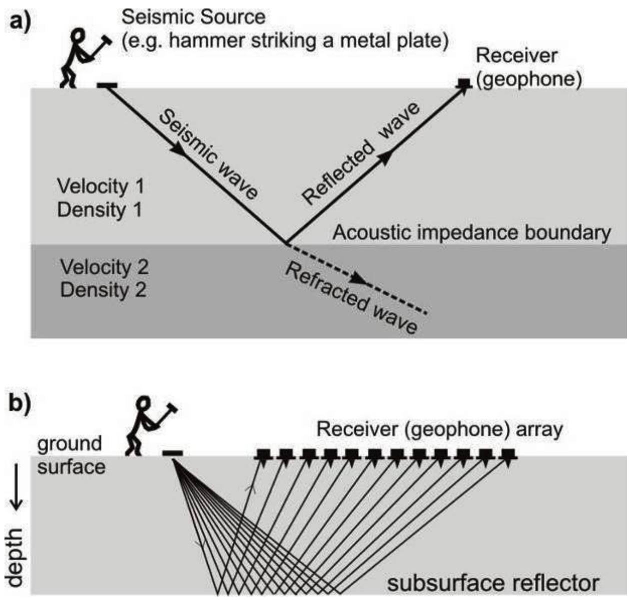

Figure 4. 6 Principle of seismic reflection.

IV.5. Recording of a seismic profile.

A seismic wave is generated by a source (S) placed at the surface. The wave propagates through the subsurface geological layers with different velocities: V_1 for the first layer and V_2 for the underlying layer ($V_2 > V_1$). The wave paths include the direct wave (T_d), the reflected wave (T_{ref}), and the refracted wave (T_r). These waves are recorded at the surface by a set of geophones (G1,G2,…,Gn) arranged at regular intervals Δx.

The depth of investigation (h) depends on the spread length (L):

- A large spread (L wide) increases penetration depth, making it possible to investigate deeper geological structures.
- A narrow spread (small L) provides closer observation points, resulting in higher resolution of wave behavior in the uppermost layer (V1).

Mathematically, the travel times can be expressed as:

Direct wave:

$$T_d(x) = \frac{x}{V_1}$$

Reflected wave:

$$T_{ref}(x) = \frac{2}{V_1}\sqrt{h^2 + \left(\frac{x}{2}\right)^2}$$

Refracted wave:

$$T_r(x) = \frac{2h\cos i_c}{V_1} + \frac{x}{V_2}$$ with $\sin i_c = \frac{V_1}{V_2}$ being the critical angle.

This setup makes it possible to determine the velocity structure, layer thickness, and geometry of geological horizons from the recorded time–distance curves.

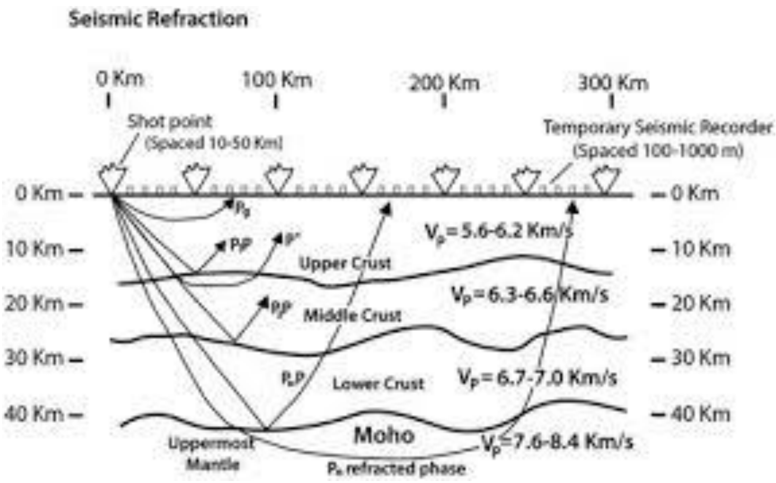

Figure 4. 7 Principle of acquisition of the seismic refraction method

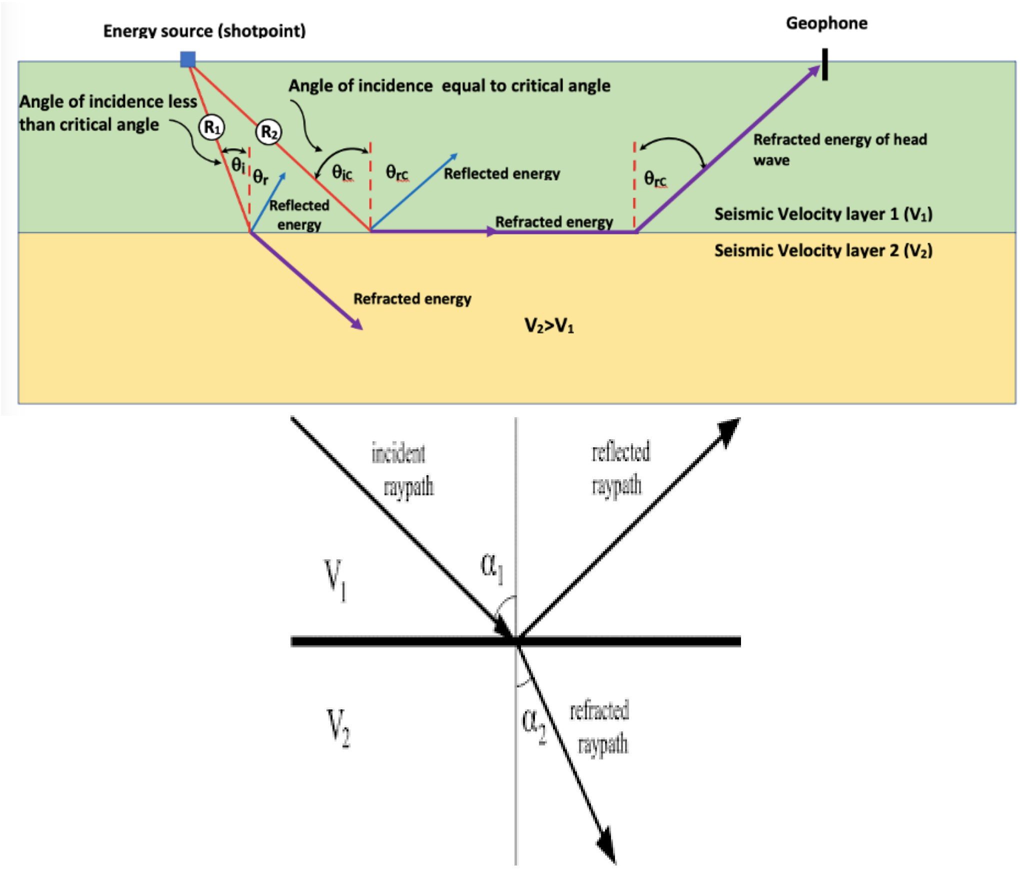

Figure 4. 8 Path of seismic waves, wavefront, and seismic rays.

IV.6. Snell–Descartes Laws

The Snell–Descartes laws describe how seismic waves behave when they encounter an interface between two media of different velocities. The law of reflection states that the angle of incidence i is equal to the angle of reflection r. The law of refraction, also known as Snell's law, is expressed as:

$$\frac{\sin i}{V_1} = \frac{\sin r}{V_2}$$

Where V_1 and V_2 are the propagation velocities in the first and second medium respectively, " i " is the angle of incidence, and " r " is the angle of refraction. When the second medium is faster ($V_2 > V_1$), a critical angle i_c appears, defined by:

$$\sin i_c = \frac{V_1}{V_2}$$

at this angle, the refracted wave travels along the interface as a head wave. If the incidence exceeds this angle, no refraction occurs and the wave undergoes total internal reflection within the first medium. These principles are fundamental in seismic refraction methods, as they explain the generation and detection of refracted waves used to investigate subsurface structures.

IV.7. Types of Seismic Methods

IV.7.1. Seismic Refraction

The seismic refraction method is a geophysical technique used to determine the velocity of seismic waves in the subsurface and to identify geological boundaries. When a seismic source at the surface (hammer, explosive, weight drop, or vibroseis) generates energy, the waves travel through the first layer with a velocity V_1. If they encounter a deeper layer where the velocity is higher ($V_2>V_1$), part of the energy is refracted along the boundary before reemerging at the surface and being detected by geophones.

Geophones, positioned at regular intervals, record the arrival time ttt of the seismic waves. By comparing the distances covered (x) with the recorded times, geophysicists build travel-time curves that distinguish different types of waves:

- **Direct waves** traveling only in the first layer (V_1),
- **Refracted waves** that bend along deeper interfaces ($V_2,V_3,\ldots$).
- Occasionally, **reflected waves** returning from layer boundaries.

From the shape of these curves, it is possible to estimate the average seismic velocities (V_1,V_2,V_3) and the thicknesses of the layers ($h_1,h_2,\ldots$). A velocity contrast ($V_{n+1}>V_n$) usually indicates a geological interface, such as the transition between soil and bedrock or between two different rock types.

The interpretation of seismic refraction data, after inversion, provides a model of the subsurface structure: the number of layers, their thicknesses, and their physical properties. This makes the method especially valuable in engineering geology (depth to bedrock), hydrogeology (detection of aquifers and impermeable layers), and environmental studies (shallow subsurface mapping). However, its limitations include reduced effectiveness in complex geology or in cases where velocity decreases with depth.

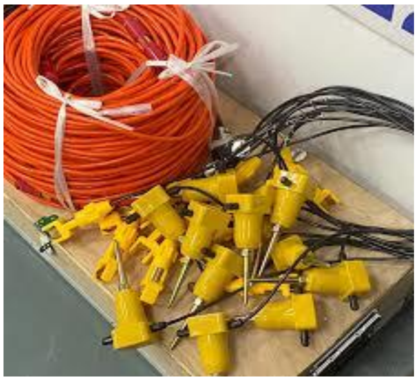

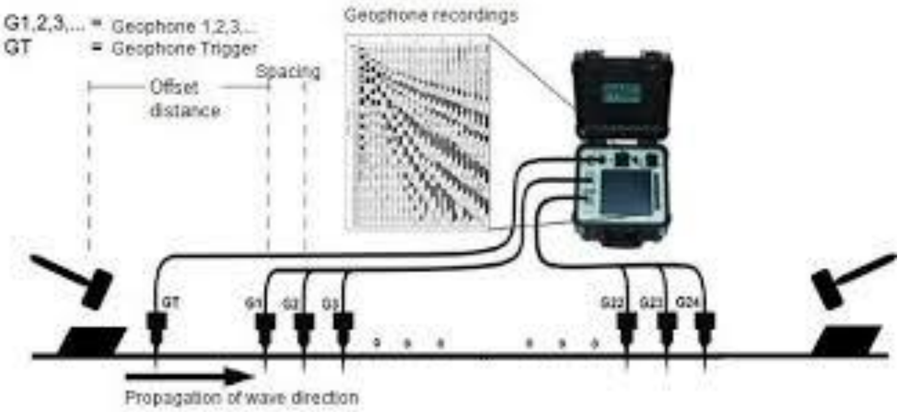
G1,2,3,... = Geophone 1,2,3,...
GT = Geophone Trigger
Geophone recordings
Offset distance
Spacing
GT
G1
G2
G3
G22
G23
G24
Propagation of wave direction

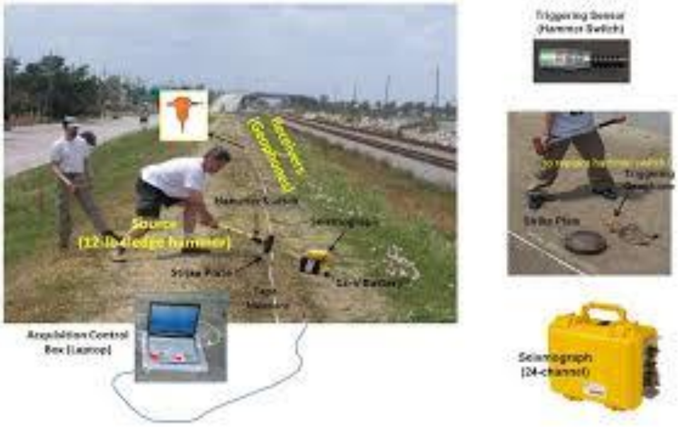
Seismograph (24-channel)


a

IV.7.2. Seismic Reflection

The seismic reflection method is one of the most powerful techniques for imaging the subsurface. It is based on the principle that when a seismic wave encounters a boundary between two media with contrasting properties, part of the energy is reflected back to the surface. The time taken by this reflected wave to return, called the two-way travel time (t_0), depends on the velocity of the medium (V) and the depth of the reflector (z).

In practice, a seismic source at the surface generates elastic waves that penetrate the ground. These waves interact with subsurface interfaces (for example, between sedimentary layers or between sediments and basement rock). Each time a significant velocity contrast exists (V_1,V_2,V_3,…), a reflection occurs. The reflected signals are detected by a dense array of geophones or seismometers, which record the arrival times and amplitudes of the returning waves.

The recorded data are displayed as a seismic section, where the vertical axis is the two-way travel time (t_0) and the horizontal axis is the position along the profile (x). Strong reflectors correspond to boundaries with large changes in acoustic impedance, which is the product of velocity (V) and density (ρ) of the material. Thus, seismic reflection provides detailed information about the geometry of layers, their depth (z), thickness (h), and internal structure.

This method is particularly valuable for mapping complex subsurface features, such as faults, folds, reservoirs, and stratigraphic sequences. It is the most widely used seismic technique in petroleum exploration, hydrocarbon reservoir characterization, and large-scale geological studies. Compared to seismic refraction, seismic reflection offers much higher resolution and can image both horizontal and steeply dipping structures. However, it requires more sophisticated acquisition systems, advanced processing steps, and often higher costs.

Chapter.5 Electromagnetic methods

V.1. Introduction

Electromagnetic (EM) methods are geophysical techniques that explore the subsurface by measuring the interaction between artificially generated or naturally occurring electromagnetic fields and the Earth's materials. These methods rely on the contrasts in **electrical conductivity (σ)**, **magnetic permeability (μ)**, and **dielectric permittivity (ε)** of rocks, soils, and fluids.

When an electromagnetic field is introduced into the ground, conductive materials such as clays, saline groundwater, or metallic mineral deposits allow the flow of **induced currents** (often called *eddy currents*). These currents generate their own secondary EM fields, which can be detected at the surface. By analyzing the characteristics of these secondary responses, geophysicists can infer the electrical properties and distribution of subsurface layers.

Electromagnetic methods are highly versatile and are applied in:

- **Mineral exploration** (detection of massive sulfides, graphite, or other conductors).
- **Hydrogeology** (aquifer mapping, groundwater salinity, freshwater–saltwater interface).
- **Environmental studies** (landfill monitoring, contamination plumes).
- **Engineering and geotechnical investigations** (bedrock mapping, utility detection).
- **Archaeological prospection** (shallow buried structures).

The main strength of EM methods lies in their non-invasive character, rapid data acquisition, and variable depth penetration, ranging from a few meters in near-surface surveys to hundreds of kilometers in deep magnetotelluric studies. However, they are also sensitive to cultural noise (e.g., power lines, fences), and interpretation often requires careful processing and inversion.

V.2. Basic Electromagnetic theory

Electromagnetic theory was first formalised by Maxwell who recognized that Ohm's law, Faraday's law, and Ampere's law were all part of a great whole, that now being called Maxwell's equations. These equations are the quintessence of the development of electromagnetic theory. Further development was only a matter of performing the appropriate mathematical manipulations. Maxwell's field equations for a homogeneous isotropic medium, assuming a time dependence of the type e iwt and a charge free space, are;

$$\nabla . E = -\partial B / \partial t$$

$$\nabla . H = J + \partial D / \partial t$$
$$\nabla . B = 0$$
$$\nabla . D = 0$$

where E is the electric field intensity (V/m), H is the magnetic field intensity (A/m), B is the magnetic induction (W/m), D is the displacement current (C/m), and J is the current density (A/m^2).

To relate Maxwell's equations to properties of the subsurface, the constitutive equations must be used

$$D = \varepsilon . E$$

$$B = \mu . H$$

$$J = \sigma . E,$$

Where ε (F/m) is the dielectric constant or electrical permitivity, μ is the magnetic permeability in ($\mu_0 = 4\pi \times 10^{*7}$ H/m free space), σ(S/m) is the electrical conductivity. In most materials μ, do not differ appreciably from the values of μ_0 and ε_0 in free space. A combination of Maxwell's and constitutive equations form a single characteristic of the medium referred to as the wave number which then determines the behavior of the EM field. Reformulation of Maxwell equations in terms of the magnetic and electrical field strengths, gives the following;

$$\nabla \times H = \sigma E + \frac{\partial}{\partial t}(\varepsilon E)$$

$$\nabla \times E = -\frac{\partial}{\partial t}(\mu H) .$$

The ratio of electric field strength to the magnetic field strength is known as the Cagniard impedance or wave impedance (units in ohm) and is given by

$$|Z| = \left|\frac{Ex}{Hy}\right| = \left(\rho \mu_0 w\right)^{1/2} = \frac{2\pi}{10^3}\left(\frac{\rho}{5T}\right)^{1/2} .$$

Re-arranging the above equation, the apparent resistivity in a homogeneous medium is

$$\rho_a = 0.2T\left|\frac{Ex}{Hy}\right|^2 .$$

The depth z at which the amplitude of the field has been attenuated by 1/e or 0.37 of its value at the surface of the medium is called skin depth and is given by

$$\delta = \frac{1}{real(k)} = \sqrt{\frac{2}{w.\mu.\sigma}} = \left(\frac{2\rho}{w\mu\sigma}\right)^{1/2} \cong 503(\rho T)^{1/2}(m).$$

The effect of conductivity on penetration depth (Fig.) can be explained physically as follow (Zhdanov & Keller, 1994): as an electromagnetic field penetrates a conductor, its energy is expended on the vibration of free electrical charge carriers present in the conductor. The vibration excited by the electromagnetic field represents conversion of the energy of electromagnetic field to heat. As a result, the field in a conductor loses energy rapidly as it travels, and is attenuated. When an electromagnetic field travels into an extensive conductor, its energy is almost entirely lost in a zone near the entry surface; this zone is like a skin protecting the interior of the conductor from penetration by electromagnetic field, and hence the name skin effect. In an insulator, there are no free charge carriers to vibrate and extract energy from the electromagnetic field, and so, the field can propagate to greater distance.

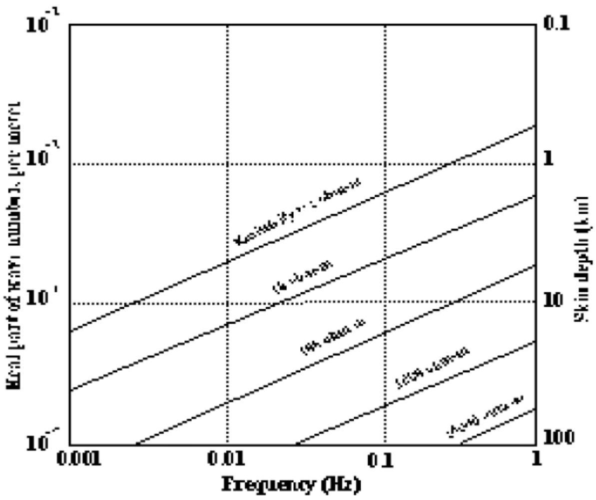

Figure 5. 1 Wave numbers as a function of frequency and resistivity.

V.3. The physical meaning of Frequency domain electromagnetic methods

The physical meaning is that a transmitter coil radiates an electromagnetic field which induces eddy currents in the subsurface. The eddy currents, in turn, induce a secondary electromagnetic field. The secondary field is then intercepted by a receiver coil. The voltage measured in the receiver coil is related to the subsurface conductivity. These conductivity readings can then be related to subsurface conditions. Figure presents a schematic drawing of EM operating principles.

The conductivity of geologic materials is highly dependent upon the water content and the concentration of dissolved electrolytes. Clays and silts typically exhibit higher conductivity values because they contain a relatively large number of ions. Sands and gravels typically have fewer free ions in a saturated environment and, therefore, have lower conductivities.

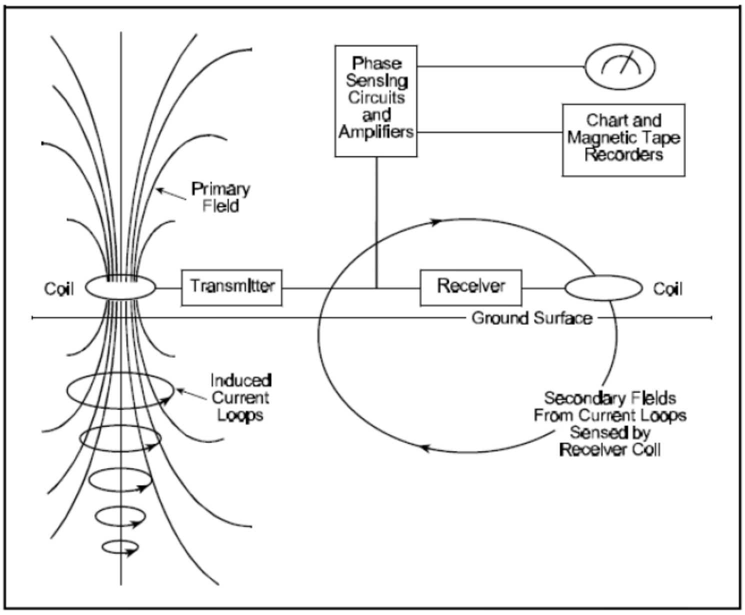

Figure 5. 2 Schematic Drawing of Electromagnetic Operating Principles

V.4. Transient electromagnetic (TEM) method

V.4.1. Basic principles

The transient electromagnetic (TEM) method is an inductive method that utilizes a strong current which is passed through a rectangular loop commonly laid on the surface of the ground. The flow of this current in the surface loop will create a magnetic field that spreads out into the ground in the form of a primary magnetic field and induces eddy currents in the subsurface. When the current is abruptly terminated, this primary magnetic field is time varying and in accordance with Faraday's law, there will be an electromagnetic induction during this time. This electromagnetic induction in turn results in eddy current flow in the subsurface. The intensity of these currents at a certain time and depth depends on ground resistivity (Kaufman & Keller, 1983), in other words, the conductivity, size, and shape of subsurface conductor. The voltage response, which is proportional to the time rate of change of the secondary magnetic field created by the eddy currents, is measured. For poor conductors, these initial voltages are large but the fields decay rapidly. For good conductors, the initial voltages are smaller but the field **decays**

slowly. Nabighian (1979) has shown that at any given time after switch off, this system of induced currents can be represented by a simple current filament of the same shape as the transmitter loop, and moves outward and downward with decreasing velocity and diminishing amplitude with time (Figure.). This is known as the smoke ring.

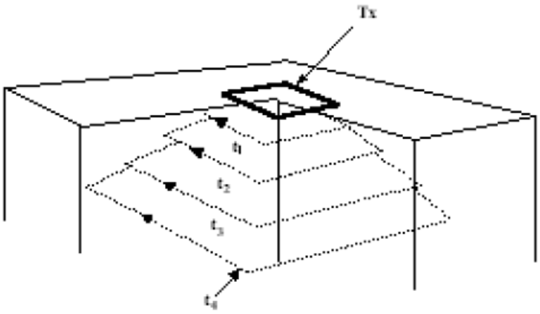

Figure 5. 3 System of equivalent current filaments at various times after current interruption in the transmitter loop, showing their downward and outward movement ((McNeill, 1990)).

The velocity with which the ring expands away from the transmitter, at a time t is given by the equation (Nabighian, 1979)

$$V_z = \frac{2}{\sqrt{\pi\sigma\mu t}},$$

and the diffusion depth, d, of the wave is given by

$$d = 2\pi\sqrt{\frac{2t}{\mu\sigma}}.$$

The depth of investigation is determined by the time interval after the transmitter current is turned off and the subsurface conductivity (equation 3.2). As the time increases, the current intensity migrates to greater depths.

The current driven through the transmitter loop consists of equal periods of on-time and off-time (Figure). The TDEM signal is measured during the transmitter off time period only, i.e. in the absence of a primary field. When the TEM response is plotted logarithmically against the logarithm of time in a homogeneous medium, the response **can** be divided into three stages, early stage (where the response is constant with time), an intermediate stage (response shape is continually varying with time), and late stage (response is a straight line).

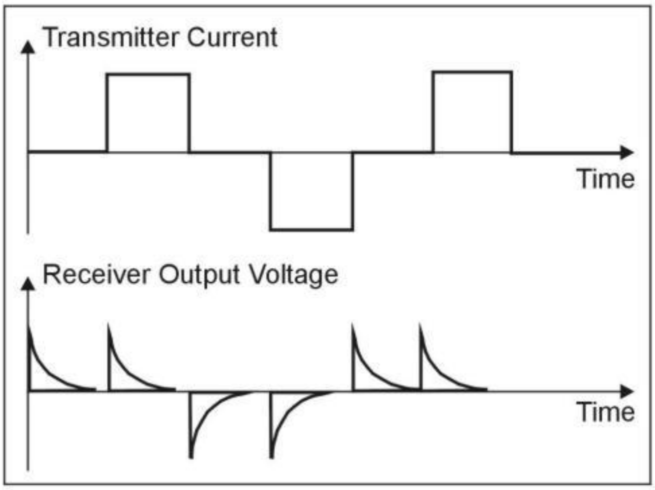

Figure 5. 4 Schematic diagram showing on and transmitter current linear ramp turn-off time and receiver signal

In the early time stage of the transient process, the induced currents (Grant & West, 1965) will be independent of the conductivity and firstly (i.e. at time t=0) be confined to the surface of the conductor in such a way as to preserve the normal component of the pre-existing primary magnetic field at the surface of the conductor (Zhdanov, 2010). At this stage, the initial current distribution is only a function of the size and shape of the conductor (Grant & West, 1965). In the subsurface, an inward diffusion of the current pattern later occurs as a result of ohmic losses which leads to the region immediately inside the conductor seeing a decreasing magnetic field and an induced emf that causes new current to flow. This is the intermediate stage. This continues until a stage is reached at which current distribution becomes more or less invariant with time. The inductance and resistance of each current ring have reached stabilised values and both the currents and their associated external magnetic fields begin to decay with a time constant given by

$$\tau = \frac{\sigma\mu a^2}{\pi^2},$$

where *a* is the radius of an equivalent circular loop.

This is the late–time stage of the transient process.

TEM in homogeneous medium

The derivative of the vertical magnetic field, as a function of time is given by (Hatch, 2017) B_Z

$$\frac{\partial B}{\partial t} = \left(\mu M / 4\pi t^{3/2}\right)\frac{(\mu\sigma)^{3/2}}{t^{5/2}}$$

Re-arranging this equation by inversion, we have

$$\rho_a(t) = \left(\frac{\mu}{4\pi t}\right)\left(\frac{2\mu M}{5tB_z^{\bullet}}\right)^{2/3}$$

where is the transmitter dipole moment, M

$B_z^{\bullet} = \frac{\partial B}{\partial t}$ and ρ_a is the apparent resistivity of the ground.

V.4.2. TEM field measurements

In the TEM survey, the transmitter is connected to a loop of wire laid on the ground. With the exception of the on time measuring system (UTEM and INPUT), all TEM transmitters generate a bipolar waveform with a ramp turn-off time as shown in Figure . The decaying voltage in the receiver is measured when the transmitter is turned off which allows the very small voltage to be measured without interference from the large primary field. The receiver samples the amplitude of the transient decay using a number of gates. The width of gates increases with time so the early time gates are narrow in order to accurately measure the voltage while the later gates, situated where the transient varies more slowly, are much broader. This wider gate enhances the signal to noise ratio which decreases with time as the amplitude of the signal decays.

The design of TEM survey depends on the depth of investigation required. The practical limitation on the depth of investigation for TEM system is determined by the maximum recording time, the time t at which the signal decays to the noise level, the source moment and earth resistivity. These independent parameters render the depth of investigation difficult to quantify. Spies (1989) has studied the depth of investigation of TEM survey; he has shown that in case of transmitter-receiver separation or loop size less than the depth of investigation (near-zone) and induced voltage measured with an induction coil, the depth of investigation is proportional to the 1/5 power of the source moment and ground resistivity . On the other hand, if the receiver is a magnetometer the depth of investigation is proportional to the 1/3 power of the source moment and is no longer a function of resistivity. In case of loop size greater than the depth of investigation (far-zone), the depth of investigation for an induced voltage receiver is proportional to the ¼ power of the source moment and resistivity and is inversely proportional to the source-receiver separation. This analysis gives the maximum depth of investigation based on detection of a buried layer. The minimum depth, at which individual conductivity variations can be resolved, is determined by the earliest sample time.

V.4.3. TEM loop configurations

The most common factor for designing all time domain techniques is the fact that they all utilize either square shaped or rectangular as the transmitter. Also a large transmitter loop offers a better capability for depth penetration. These methods use either fixed- or moving-loop configurations and measure the rate of decay of the secondary field when the primary field is switched off. They are mostly used to investigate the variation of conductivity with depth (resistivity sounding). A number of different loop configurations are possible for TEM measurements, some being better than others for specific geologic situations. They include the common zero-offset (in-loop and single-loop), short offset (separated-loop or soTEM) and the long-offset (loTEM) techniques. Figure 5.5 illustrates the most common loop configurations. Brief descriptions of the most commonly used TEM loop configurations are given below.

Central loop (or in-loop) configuration:

In this method, a dipole multi turn receiver is located at the center of the transmitter loop. The size of transmitter loop varies between 50 x 50 and 500 x 500 m depending upon the exploration depth required. The rule of thumb is that the transmitter size is approximately one half the depth of penetration. The receiver coil is much smaller (usually a multi turn coil of 1 m diameter). Several different receivers can be used consecutively to record the transient over a large dynamic range with better resolution. Shallow anomalies near the centre of the loop are expected to have a large effect on the central receiver. The advantage of on-loop technique is that it gives high resolution of conductor position, provided in homogeneities are minimal, and provides horizontal as well as vertical components of the magnetic field.

Coincident (transmitter-receiver) loop or single loop:

This configuration utilizes a single loop both as a transmitter and a receiver. The loop acts as transmitter when the current is in the loop and as a receiver once the current is switched off. Coincident transmitter-receiver loop has the same geometry and response as the single loop configuration except that the transmitter and receiver are separate loops laid out spatially coincident. This loop is widely used in the search for large stratiform targets at depth since the propagation distances to and from the

target are minimised, resulting in less signal attenuation of both primary and secondary fields. Further, the secondary field effects are purely additives. This simplifies interpretation and facilitates the detection of weak secondary signals. **Common sizes are 50, 100 or 200 m per side.** Loops smaller than 50 m per side may require more than one turn to give effective dipole moments but such loops can be time consuming to lie out. Depth of penetration increases with increasing loop size and is 2-3 times the loop side length or more. The advantage of this loop is its highest signal level because the receiver loop is in place of strongest transmission especially when the transmission field is attenuated by conductive overburden. This also ensures a degree of coupling with targets at any orientation especially if they lie at a near horizontal attitude.

Offset loop:

It consists of a large transmitter loop that can have sides up to 1km long. A small roving receiver is moved both inside and outside the Tx loop along lines that are perpendicular to the side of the loop. The main advantage of this is its greater depth of penetration and high productivity but some consideration must be taken into account from erroneous interpretation due to current gathering and channeling phenomena that occur, especially in conductive terrain (Spies and Parker, 1984).

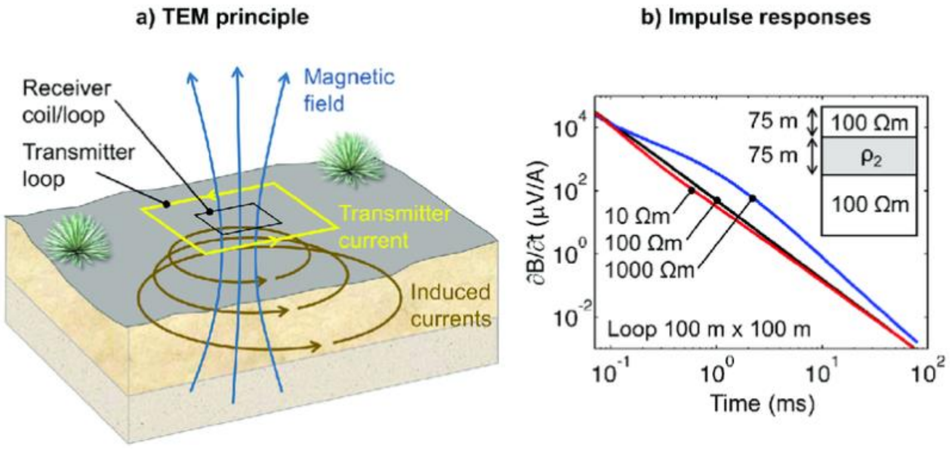

Figure 5. 5 TEM loop configurations.

V.5. Ground Penetrating Radar (GPR)

Ground Penetrating Radar (GPR) uses high-frequency electromagnetic waves (10–3000 MHz) to image the subsurface. An antenna emits radar pulses, which reflect back when encountering subsurface objects, creating high-resolution profiles. Higher frequencies give better resolution but shallower penetration, while lower frequencies penetrate deeper with less detail. Penetration depth also depends on soil conductivity: conductive materials (wet clays, saline soils) strongly attenuate signals, often limiting depth to < 0.55m, whereas dry, resistive soils (sand, gravel) allow penetration up to ~30m. Typical depths range from 1–5 m. Depths are calculated from two-way travel times of reflected waves, measured in nanoseconds.

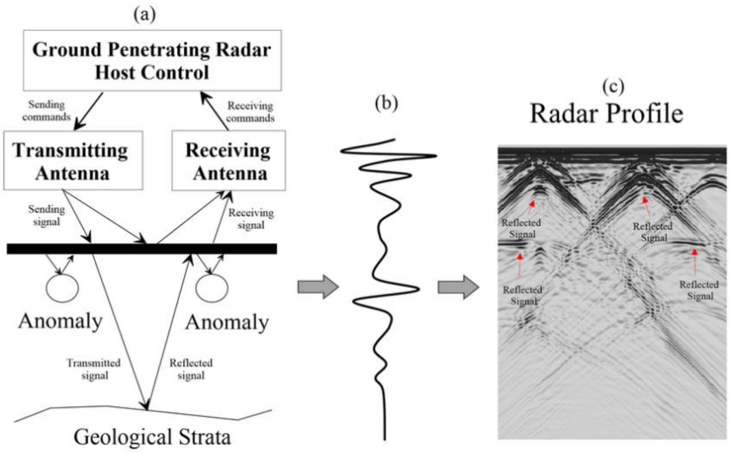

Figure 5. 6 Schematic Drawing Of Ground Penetrating Radar Operating

GPR surveys are typically conducted along parallel lines, with line spacing determined by target size and survey detail required. Traverse speeds vary: average walking pace (2–3 mph) is common, detailed surveys can be as slow as 0.1 mph, and vehicle-mounted systems can reach up to 65 mph for reconnaissance. Data may be recorded for later processing or analyzed in real time. GPR is generally unaffected by cultural noise when using shielded antennas; with unshielded antennas, skilled operators can still recognize and discount reflections from overhead objects.

V.6. Induced Polarization (IP) method

The Induced Polarization (IP) method, first observed by Conrad Schlumberger (Dobrin, 1960) as “provoked polarization,” is based on the phenomenon where the ground retains an electrical charge after a current is switched off. Instead of the potential difference dropping instantly to zero, it decays gradually, indicating that some subsurface materials can temporarily store electrical charge.

Two main approaches exist:

- Time-domain IP: studies the decay of voltage after the current is switched off.
- Frequency-domain IP: examines the decrease in apparent resistivity as current frequency increases.

IP is especially useful for exploring disseminated sulfide ore bodies. Its use in engineering and hydrogeology is more limited, though it has been applied to groundwater exploration, mainly with the time-domain technique.

V.6.1. General Theory of the IP Effect

The **Induced Polarization (IP) effect** arises when an external electric current is applied to the ground and then interrupted. Certain rocks and soils temporarily store electrical charge, causing a delayed voltage decay rather than an instantaneous drop. This behavior is explained by the interaction between the applied current and the **electrochemical properties of the subsurface**.

Key processes behind the IP effect:

1. **Electrochemical polarization**
    - Occurs at the interface between electrolytic fluids (groundwater, pore fluids) and solid grains (often metallic or clay minerals).
    - Ions accumulate at grain boundaries, forming an electrical double layer, similar to a weak battery.
2. **Membrane (or ionic) polarization**
    - Fine-grained materials like clays act as semi-permeable membranes.
    - Selective ion movement across these membranes produces charge buildup.
3. **Electrode polarization**
    - In the presence of disseminated conductive minerals (e.g., sulfides), the grains act like micro-electrodes.
    - When current is applied, charges accumulate on mineral surfaces; after current interruption, slow discharge produces measurable IP decay.

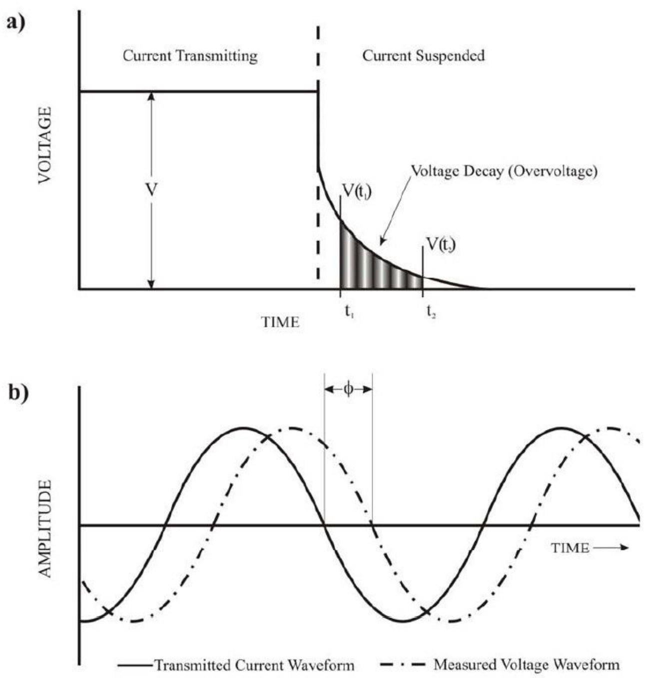

Figure 5. 7 Time domain and (b)frequency domain waveform illustrations (Glaser, 2007).

measurements

- Time-domain IP (TDIP): voltage decay after a DC current is switched off. → Measured quantity: transient voltage vs time (V(t)).
- Frequency-domain IP (FDIP) / complex resistivity (CR): amplitude and phase of voltage for sinusoidal currents at different frequencies.
  → Measured quantities: apparent resistivity $\rho_a(f)$ and phase $\varphi(f)$.

Typical field setup

- Electrodes/array: Wenner, Schlumberger, dipole–dipole, pole–dipole — choice depends on resolution vs depth.
- Current injection: large current injected between current electrodes (I), potential difference measured between potential electrodes (V).
- Acquisition: measure V while current ON (for resistivity) and record decay after current OFF (for IP).

Time-domain IP — practical parameters

Current amplitude: typically 0.5–5 A (depends on system and ground resistivity).

On/off timing: common windows: 1s on / 1s off, or longer for deep targets (e.g., 4s on / 4s off).

Delay windows: sample voltage decay in several logarithmically spaced time windows after turn-off (e.g., 1–10 ms, 10–100 ms, 100–1000 ms).

Stacking: repeat pulses and average (stack) to improve signal-to-noise ratio (SNR); typical stacks = 4–64.

Sampling: high sampling rate soon after turn-off (to capture fast decay) and progressively lower later — use log spacing.

Chargeability metrics:

Integral chargeability (area under V(t)/V_on curve over a time window).

M-values or normalized chargeability for specified windows (e.g., M0 = integral 0–50 ms, M1 = 50–300 ms).

Units: volts for V, ohm-m for resistivity, millivolt/volt or milliseconds for chargeability (often reported in mV/V or ms).

Frequency-domain IP — practical parameters

Frequencies used: from <1 Hz up to kHz (depends on target and instrument).

Measurements: amplitude ratio (apparent resistivity vs frequency) and phase shift between current and voltage.

Outputs: complex resistivity $\rho^*(f) = \rho'(f) + j\rho''(f)$; or conductivity $\sigma^*(f)$.

Resolution: FDIP gives continuous spectral behaviour, useful for petrophysical modelling.

Instrumentation & data logging

Key instrument features: programmable pulse timing, stacking, wide dynamic range, automatic electrode checks, GPS tagging, digital storage.

Common practice: log field notes (weather, electrode contact resistance, current levels, stacking count, time windows).

Processing & interpretation

Preprocessing: baseline correction, stacking, window selection, noise removal.

Inversion: convert apparent chargeability/resistivity to true distribution (1D/2D/3D inversion).

Joint interpretation: combine IP with resistivity, geology, drilling logs for robust interpretation (IP highlights polarization—often sulfides/clays; resistivity shows conductive/ resistive zones).

Petrophysical links: attempt to relate chargeability to volumetric content of metallic minerals or surface area (requires lab calibration).

Quick field checklist:

The important steps to follow in the field to make sure the equipment works and the data collected are correct are:

- Select array and electrode spacing for target depth.
- Check electrode contact resistance.
- Set current amplitude and on/off timing.
- Choose stacking and time windows (TDIP) or frequency list (FDIP).
- Run calibration / reciprocity checks.
- Record pulses, stack, and save raw V(t) or ρ*(f).
- Note environmental / cultural noise and GPS location.
- Perform at least one repeated measurement for QC.

V.7. Advantages and limitations of electromagnetic methods:

Advantages:

- Rapid data acquisition and high productivity.
- Non-invasive and cost-effective compared to drilling.
- Sensitive to conductivity variations (good for mapping groundwater, ores, contamination).
- Can detect both shallow and deep targets, depending on frequency.
- Useful in areas with difficult terrain (light equipment, portable).

Limitations:

- Strongly affected by cultural noise (power lines, pipelines, fences).
- Resolution decreases with depth.
- Interpretation can be non-unique (different subsurface models can explain same data).
- Limited penetration in highly conductive ground (e.g., clays, saline soils).
- Requires good processing and skilled interpretation to avoid errors.

References

Carmichael, R. S. (2017). *Revival: Practical Handbook of Physical Properties of Rocks and Minerals (1988)*. CRC press.

Chouteau, M. & Giroux, B. (2006). *École polytechnique montréal* 14, 149.

Clark, S. P. (1966). *Handbook of physical constants*. Geological society of America.

Dobrin, M. B. & Savit, C. H. (1960). *Introduction to geophysical prospecting*. McGraw-hill New York.

Grant, F. S. & West, G. F. (1965). *Interpretation theory in applied geophysics*. McGraw-Hill New York.

Halliday, D., Resnick, R. & Walker, J. (2013). *Fundamentals of physics*. John Wiley & Sons.

Hatch, M. (2017). *Preview* 2017, 37-38.

Kaufman, A. A. & Keller, G. V. (1983). *Chi-Yu King Roberto Scarpa* 207.

Lowrie, W. & Fichtner, A. (2020). *Fundamentals of geophysics*. Cambridge university press.

McNeill, J. D. (1990). *Geotechnical and environmental geophysics* 1, 191-218.

Nabighian, M. N. (1979). *Geophysics* 44, 1700-1705.

Sharma, P. V. (1997). *Environmental and engineering geophysics*. Cambridge university press.

Sheriff, R. E. (2002). *Encyclopedic dictionary of applied geophysics*. Society of exploration geophysicists.

Spies, B. R. (1989). *Geophysics* 54, 872-888.

Stacey, F. D. & Davis, P. M. (2008). *Physics of the Earth*. Cambridge University Press.

Telford, W. M., Geldart, L. P. & Sheriff, R. E. (1990). *Applied geophysics*. Cambridge university press.

Ward, S. (1990). *Investigations in Geophysics* 5.

Zhdanov, M. S. (2010). *Geophysics* 75, 75A49-75A66.

Zhdanov, M. S. & Keller, G. V. (1994). *Methods in geochemistry and geophysics* 31, I-IX.